

COMPUTATIONS OF AIR FILMS BETWEEN MOVING
WEBS AND SUPPORT ROLLERS

By

SATYANARAYAN KOTHARI

Bachelor of Engineering

Visvesvarayya Regional College of Engineering

Nagpur University, Nagpur, India

1993

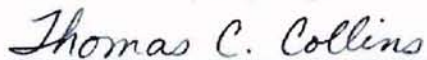
Submitted to the Faculty of the
Graduate College of the
Oklahoma State University
in partial fulfillment of
the requirements for
the Degree of
MASTER OF SCIENCE
May, 1996

COMPUTATIONS OF AIR FILMS BETWEEN MOVING
WEBS AND SUPPORT ROLLERS

Thesis Approved:



Thesis Adviser



Dean of the Graduate College

ACKNOWLEDGMENTS

I wish to express my sincere appreciation to my major advisor, Dr. F.W. Chambers, for his intelligent supervision, constructive guidance, encouragement and help during this work and during my stay at Oklahoma State University. I am also grateful to the other committee members, Dr. Peter Moretti and Dr. J. Keith Good for their suggestions and help.

More over, I wish to express my sincere gratitude to those who provided suggestions and assistance for this study. I also wish to thank my friends and colleagues at Oklahoma State University for their support and making my stay a success. Special thanks are due to the Web Handling Research Center for the financial support during the course of this work.

I am deeply indebted to my father Mr. Sunderdas Kothari, and mother Mrs. Shanta Kothari for their continued prayers, moral support and encouragement.

TABLE OF CONTENTS

Chapter	Page
I. INTRODUCTION	1
1.1 Background	1
1.2 Review of Foil Bearing Theory	4
1.3 Problem Statement	9
II. LITERATURE REVIEW	10
III. MATHEMATICAL FORMULATION	18
3.1 Problem Formulation	18
3.2 Basic Equations	18
3.2.1 Reynolds Lubrication Equation	18
3.2.2 Foil Equation of Motion	24
3.3 Governing Equations	27
3.4 Boundary Conditions	31
3.5 Initial Conditions	32
3.6 Tangency Point Location	32
IV. FINITE DIFFERENCE SOLUTION APPROACH	35
V. RESULTS	39
5.1 Results for Nonporous (infinitely wide) Webs	41
5.2 Results for Porous Webs	53
5.3 Summary	60
VI. CONCLUSIONS AND RECOMMENDATIONS	62
6.1 Conclusions	62
6.2 Recommendations for Future Work	63
SELECTED BIBLIOGRAPHY	65
APPENDIXES	70

Chapter	Page
APPENDIX A--REYNOLDS LUBRICATION EQUATION FOR NONPOROUS WEB WITH STATIONARY ROLLER	70
APPENDIX B--REYNOLDS LUBRICATION EQUATION FOR POROUS WEB WITH ROTATING ROLLER	73
APPENDIX C--FINITE DIFFERENCE FORMULATION OF THE TWO GOVERNING EQUATIONS	77
APPENDIX D--COMPUTER CODE FOR THE COMPUTATIONS OF THE AIR FILM THICKNESS AND PRESSURE DISTRIBUTION	81

LIST OF FIGURES

Figure	Page
1.1 Schematic of Typical Continuous Web Loop	2
1.2 Three Dimensional Schematic of Foil Bearing	5
1.3 Two Dimensional Schematic of Foil Bearing	6
2.1 Magnetic Tape Being Wound Onto Tape Pack Under Tension T With Tape Speed V	17
3.1 Differential Fluid Element for Dynamic Equilibrium Analysis	20
3.2 Differential Element for Conservation of Mass Analysis for Nonporous Foil	23
3.3 Differential Foil Element	25
3.4 Schematic of a Web Moving Over a Roller	28
3.5 Differential Element for Conservation of Mass Analysis for Porous Foil	30
3.6 Schematic Indicating the Tangency Points for Initial Conditions	34
5.1 Transient Air Film Thickness Profiles (V=500 ft/min and T=1.58 lb/in)	42
5.2 Pressure Distribution Profiles (V=500 ft/min and T=1.58 lb/in)	42
5.3 Comparison of Air Film Thickness With and Without Slip Flow for Low Web Velocity (V=500 ft/min and T=1.58 lb/in)	44
5.4 Comparison of Air Film Thickness With and Without Slip Flow for High Web Velocity (V=2500 ft/min and T=1.58 lb/in)	44

Figure	Page
5.5 Combined Air Film Thickness Profile and Pressure Distribution Profile (V=500 ft/min and T=1.58 lb/in)	45
5.6 Transient Air Film Thickness Profiles (V=1000 ft/min and T=1.5 lb/in)	48
5.7 Transient Air Film Thickness Profiles (V=3000 ft/min and T=1.5 lb/in)	48
5.8 Air Film Gap With Varying Tension (V=3000 ft/min)	49
5.9 Air Film Thickness With Varying Web Velocity (T=1.5 lb/in)	49
5.10 Steady State Air Film Thickness for Varying Web Mass (V=1000 ft/min and T=1.5 lb/in)	50
5.11 Air Film Thickness Profiles (Central Region) With Increasing Mass (V=1000 ft/min and T=1.5 lb/in)	50
5.12 Steady State Air Film Thickness for Varying Web Mass (V=3000 ft/min and T=1.5 lb/in)	51
5.13 Air Film Thickness Profiles (Central Region) With Increasing Mass (V=3000 ft/min and T=1.5 lb/in)	51
5.14 Comparison of Steady State Air Film Gap for Stationary and Rotating Roller (V=3000 ft/min and T=1.5 lb/in)	52
5.15 Steady State Air Film Thickness Profiles for Porous Web With Varying Tension (V=2008 ft/min and $K=0.3e-5 (m^3/s)/(m^2-Pa)$)	56
5.16 Steady State Air Film Thickness Profiles for Porous Web With Varying Velocity (T=0.71 lb/in and $K=0.3e-5 (m^3/s)/(m^2-Pa)$)	56
5.17 Comparison of the Air Film Thickness Profile for Porous Web (Central Region) (V=2008 ft/min, T=0.71 lb/in and $K=0.3e-5 (m^3/s)/(m^2-Pa)$)	57
5.18 Comparison of the Air Film Thickness Profile for Porous Web (Central Region) (V=2500 ft/min, T=0.71 lb/in and $K=0.3e-5 (m^3/s)/(m^2-Pa)$)	57
5.19 Comparison of the Air Film Thickness Profile for Porous Web (Central Region) (V=2992 ft/min, T=0.5 lb/in and $K=0.52e-5 (m^3/s)/(m^2-Pa)$)	58

Figure	Page
5.20 Comparison of Exit Region Air Film Thickness Profile for Nonporous and Porous ($K=0.3e-5 \text{ (m}^3/\text{s)/(\text{m}^2\text{-Pa)}$) Web ($V=2008 \text{ ft/min}$ and $T=0.71 \text{ lb/in}$)	59
5.21 Comparison of Exit Region Air Film Thickness Profile for Nonporous and Porous ($K=0.52e-5 \text{ (m}^3/\text{s)/(\text{m}^2\text{-Pa)}$) Web ($V=2992 \text{ ft/min}$ and $T=0.5 \text{ lb/in}$)	59

NOMENCLATURE

b	web thickness
C_1, C_2	constants of integration
E	modulus of elasticity
F	force
F_s	shear
h	air film thickness
h_0	constant central region (also initial) air film thickness
i	subscript indicating position in x direction (along roller)
I	moment of inertia of web cross-section
k	permeability coefficient of porous web
K	permeability of porous web
L	distance between the two end supports
L_1, L_2	location (x coordinates) of points on the roller within which tangency points are located
m	mass
M	moment
n	superscript indicating time step
p	pressure
p_a	ambient pressure

p_0	initial pressure in air bearing region
Q	mass flow rate
R	roller radius
T	web tension
t	time
V	velocity
V_R	roller surface velocity
V_t	velocity of the air escaping through the porous web
V_w	web velocity
w	half width of the web
x	spatial coordinate along the direction of web velocity
y	spatial coordinate along radial direction i.e. along web displacement
z	spatial coordinate along the width of the web
$\delta(x)$	function describing roller surface geometry
λ	mean free path length
λ_a	mean free path length at atmospheric pressure
μ	dynamic viscosity of air
ν	kinematic viscosity of air
ρ	web density
τ	viscous shear stress

CHAPTER I

INTRODUCTION

1.1 Background

A web is defined as a material manufactured in continuous strip forms. This definition of web envelopes a wide range of products, for example, plastic films, paper rolls, printing applications, textiles, magnetic tapes, etc. . The materials processed as webs demand techniques for their effective transportation during the processing and physical treatments. These techniques may be collectively termed as web handling.

In modern web handling applications webs are pulled at high speeds over the surfaces of guide and drive rollers as shown in Figure 1.1. This action results in a self-acting air bearing which helps to reduce the wear by separating the web from the roller by a thin air film. The air film gap on which the web flies must be thick enough to prevent excessive abrasion under all operating conditions, yet it must be thin enough to allow sufficient asperity contact for maintaining the traction and preventing any lateral wandering of the web. Excess air wound into a roll also leads to trapped air defects such as “telescoping” and the deterioration of roll mechanical properties. As the air film gap increases to a height greater than the asperity heights of the web and roller, a loss in web-roller traction can be expected. Thus much attention has been devoted in recent years to analytical and numerical methods which will predict the web-roller separation and serve as an aid in roller design and suggest measures to control this separation effectively.

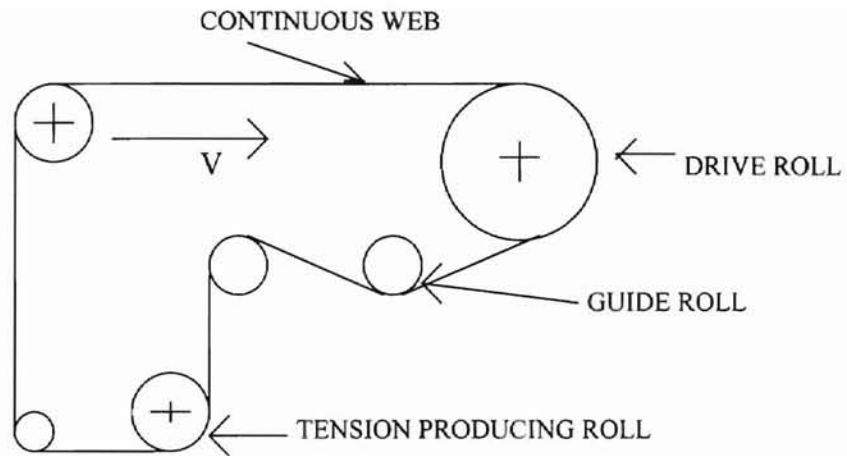


Figure 1.1: Schematic of Typical Continuous web Loop

According to the investigations carried out by Daly [1965] the significant variables effecting the traction between the webs and their carrying rolls are:

1. Web speed
2. Web tension
3. Web porosity
4. Wrap angle
5. Roll diameter
6. Web moisture
7. Paper grade

the last two being specifically considered for paper-related or other porous web applications.

The higher the speed, the more air is entrained into the gap between the web and the roller. Progressively the web loses the traction with the roller which moves them at the same velocity. On the other hand an increase in tension increases the traction between the web and the roller. Daly showed that the web traction increases with an increase in wrap. For porous webs, traction increases with increase in roller diameter as the porous webs did not develop large air films due to air leakage through the web. For nonporous webs the traction decreases as the roller diameter increases because larger rollers generate thicker air films and there is no passage for trapped air through the nonporous webs.

Due to the finite viscosity of air and the no-slip condition at the surfaces of the roller and web, air is forced to the point where the web approaches the roller. This trapped air escapes from the exit region and due to the squeeze film effect some of the air

is forced to escape in the spanwise (lateral) direction. Thus in order to improve the machine performance for high speed operation, the estimation of the air entrainment is very essential.

From the foregoing discussion, the importance of the web-air-roller interaction can be easily recognized and is one of the major concerns for the industrial practitioners. Knox and Sweeney [1971] provided some insight regarding air entrainment in winding applications. The authors suggested the application of foil bearing theory to model air entrainment effects in winding because of the geometrical similarity between the two problems. Based upon their analysis an expression for nominal air thickness was obtained.

1.2 Review of Foil Bearing theory

It is appropriate next to review the foil bearing theory. As shown in Figure 1.2 and Figure 1.3 a foil bearing consists of a rotating shaft which is supported by a stationary foil. Alternately, the shaft may be stationary and the foil moving. The angle of wrap may vary over a range of 0 to 180 degrees or more. The film is developed by the fluid entrainment due to the motion of one or both of the surfaces.

Gross [1980] presented the design of foil bearings based on the simultaneous solution of the equation describing the behavior of both the fluid and the foil itself. The Reynolds equation relates the pressure in the fluid film to the film thickness, to the speed, and to the lubricant viscosity. The foil equilibrium equation relates the elastic properties of the foil to the tension and pressure on the foil. The Reynolds equation is-

$$\frac{\partial}{\partial x} \left(h^3 p \frac{\partial \phi}{\partial x} \right) + \frac{\partial}{\partial z} \left(h^3 p \frac{\partial \phi}{\partial z} \right) = 6\mu V \frac{\partial \phi}{\partial x} + 12\mu \frac{\partial \phi}{\partial t} \quad (1.1)$$

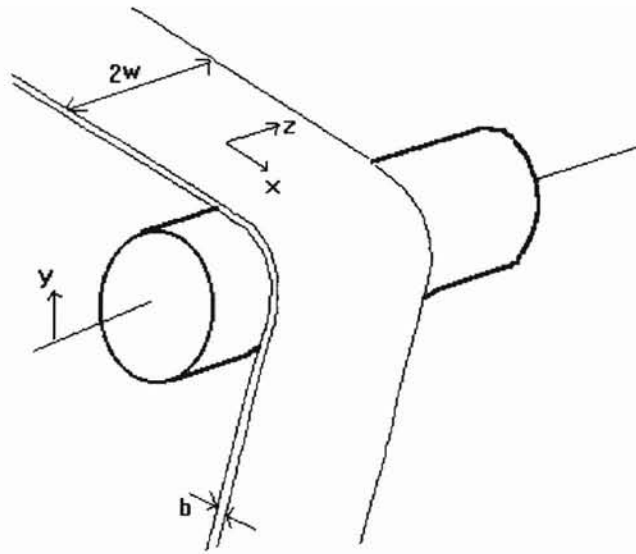


Figure 1.2 : Three Dimensional Schematic of Foil Bearing

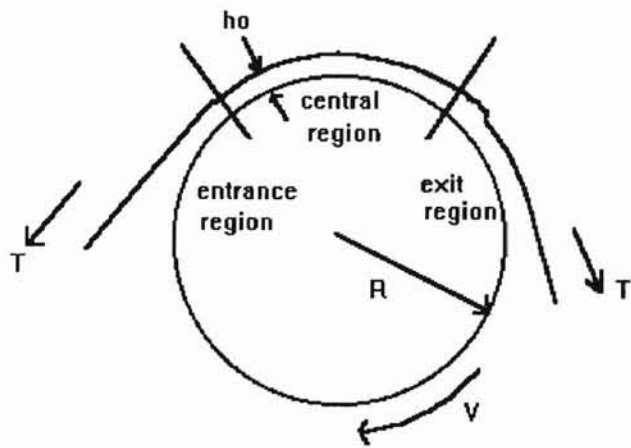


Figure 1.3 : Two Dimensional Schematic of Foil Bearing

For a perfectly flexible foil with an incompressible lubricant, infinite width and steady characteristics in time, the Reynolds equation reduces to

$$\frac{\partial}{\partial x} \left(h^3 \frac{\partial p}{\partial x} \right) = 6\mu V \frac{\partial h}{\partial x} \quad (1.2)$$

The equilibrium equation for a foil can be derived by setting up the stress, strain, and bending moment resultants. The equilibrium equation is-

$$\frac{Et^3}{12(1-\nu^2)} \nabla^2 \nabla^2 h + \frac{Et(h-h_0)}{R^2} = p - p_0 - \frac{T}{R} \left(1 - R \frac{\partial^2 h}{\partial x^2} \right) \quad (1.3)^*$$

For a perfectly flexible foil the bending terms in the equilibrium equation can be neglected with respect to the tension terms reducing the equilibrium equation to

$$(p - p_0) = \frac{T}{R} \left(1 - R \frac{\partial^2 h}{\partial x^2} \right) \quad (1.4)$$

combining the two simplified equations we obtain an equation called the **foil bearing equation**, which is

$$\frac{\partial}{\partial x} \left(h^3 \frac{\partial^3 h}{\partial x^3} \right) = -\frac{6\mu V}{T} \frac{\partial h}{\partial x} \quad (1.5)$$

To obtain the solution Gross developed a nondimensional form of the equation using nondimensional variables and performed a simple linearization after integrating once.

In the entrance region (Refer to Figure 1.3) pressure increases from ambient to the film pressure, P and a decrease in air gap occurs smoothly and is exponential in form. Next comes the central constant gap region. The gap, h_0 and pressure, P remain constant for this region. The last region is the exit region where pressure decreases from P to

* ν in the equation is the Poisson's Ratio and not the kinematic viscosity of air

ambient pressure while the gap increases from h_o to infinity. From the Reynolds equation it is obvious that a negative pressure gradient can exist only if the air gap at the exit is less than h_o , which is incompatible with an increasing gap. The increase in gap is therefore preceded by a region where the air gap is less than h_o in which pressure decreases to below ambient followed by a region of increasing gap and increasing pressure.

For a self-acting foil bearing the air film height in the constant gap central region is given by-

$$h_o = KR \left(\frac{6\mu V}{T} \right)^{2/3} \quad (1.6)$$

where $K = 0.643$, but different researchers have proposed slightly different values for “K”. Basheer [1988] based on his experimental work recommended the use of $K=0.706$ to find the air-film thickness in high speed cases. Knox and Sweeney [1971] proposed a change in equation (1.6) for application to web handling. They suggested that for a system in which both the foil and the surface are in motion the more general form for the constant gap film height will be-

$$h_o = 0.643R \left[\frac{6\mu(V_{web} + V_{roller})}{T} \right]^{2/3} \quad (1.7)$$

The above equation was based on the assumption that the width of the web is infinite and there is no air flow in the spanwise direction. This also suggests that the pressure remains constant along the width of the web. However in the actual conditions of a finite width web the pressure must decrease from the pressure in the constant gap region to the

ambient pressure near the edges of the web. The effect of this negative pressure gradient may be a decrease in air film gap from the center of the web towards its edges.

1.3 Problem Statement

It may be inferred from the foregoing discussion that the need for predicting the air film thickness between the web and roller must be very well realized. It is also apparent that the prediction of the air film thickness is a first step for any attempt to control and manipulate the air film thickness. Based upon the previous discussion, the primary objectives of this study are:

1. Numerically study the transient behavior of air-film thickness between a roller and a moving web.
2. Numerically study the effect of the following parameters on the air-film thickness:
 - a) Web Velocity
 - b) Web Tension
 - c) Web Mass
 - d) Slip Flow
 - e) Roller Velocity
 - f) Roller Radius.
3. For porous webs numerically study the effect of porosity on air-film thickness.

CHAPTER II

LITERATURE REVIEW

The first step in developing a numerical model to predict the air film thickness between a roller and a web is to develop governing equations describing the physical problem of a web moving over a roller. A detailed literature review suggests that most directly relevant to web handling is the problem of the air film gap between a magnetic tape and a recording head. The trend towards increased data transfer rates generally requires higher tape speeds. As these speeds increase, the hydrodynamics associated with the entrapped air layer can lead to inefficient data transfer and mechanical instability during tape winding.

Parallel is the problem of controlling the air film gap between a roller and web, and the entrapped air during web winding. Predicting the air film gap serves as a guide for controlling and manipulating the required air film gap for efficient operation. The prediction of the spacing between the head and tape requires simultaneous solution of coupled equations. One is the dynamic motion equation (equation 1.3) for the finite length of the tape or foil and the other is the transient Reynolds Lubrication equation (equation 1.1) for the air film.

Eshel and Elrod [1965] derived the differential equation applicable to the film thickness beneath an infinitely wide, perfectly flexible self-acting tape and obtained accurate numerical solutions for the film thickness in both the entrance and exit region.

Barlow [1967] developed the self-acting foil bearing equations including the compressibility of the lubricant and bending stiffness of the tape. The boundary conditions were divided equally between the two ends of the tape. He obtained the linearized solution for large wrap angles neglecting the bending stiffness of the tape. Eshel [1968] studied the effects of compressibility on an infinitely wide, perfectly flexible foil bearing. He found that with increasing compressibility, the nominal clearance decreases and the exit region undulation decreases in amplitude. The decrease is due to the smaller volume flow rate of a given mass flow for higher pressure. Eshel and Wildmann [1968] presented the unsteady problems of a foil moving along a flat, solid surface and derived an equation for the oscillations of a foil over a lubricating fluid film. Later Eshel [1969] presented a technique for the numerical solution of the time dependent foil bearing problems. Eshel [1970a] modified the foil bearing equation to include the effects of the molecular mean free path since the gaps of interest were small and investigated factors useful in overcoming excessive air gap in foil bearings. Eshel [1970b] also derived equations for a foil over a lubricating film in which the effects of fluid inertia are taken into account and obtained approximate solutions showing the effects of inertia. The effect of inertia is to considerably increase the fluid-film thickness. Knox and Sweeney [1971] were among the first to apply foil bearing theory to the problem of web handling. Previously, the theory has been applied to self-acting foil bearings in which a thin flexible medium (the foil) moves over a stationary rigid surface. Knox and Sweeney extended the analysis to the case where both the foil and the surface were moving at the same speed.

Eshel and Lowe [1973] presented a modified model of a foil bearing, taking into account some details of the particular geometry of magnetic heads and used it to predict the separation and compare it to experimental results. Dais and Barnum [1974] derived equations for the steady state problem of a foil moving relative to a drum with a geometric deviation from the perfectly circular shape. Considering an incompressible fluid and a perfectly flexible foil they presented the results for the problem of a stationary foil stretched over a rotating circular drum with a flat. Eshel [1974] analyzed the effects of external pressure exerted on foil bearings and concluded that substantial reduction in film thickness can be achieved by applying small pressures in the inlet zone. Stahl, et al. [1974] also presented a solution of the foil bearing. They retained the time derivative terms in the governing equations and accomplished the coupling by going from transient to steady state. The method was faster than the direct coupling of the equations through a standard relaxation technique. More recently Granzow and Lebeck [1984] developed a solution of the governing equations by a Crank-Nicholson form of the finite difference equations to represent the time derivative terms involved. It required the use of Newton's method to solve the system of equations at each time increment. This method allows large time steps and is fast. Brewen, et al. [1985] have developed an inverse method in which the desired spacing profile is specified and the corresponding head profile is determined, eliminating the need for iterative coupling between the tape and air bearing equations. However, this approach can result in head profiles which are difficult to manufacture. In another analysis Tanaka [1985] studied the tape spacing for a magnetic tape unit analytically and experimentally retaining the tape bending rigidity, gas

compressibility and slip flow effects. The numerical technique for calculating the tape spacing uses an influence coefficient method for the tape equation and the Newton-Raphson iterative method for the Reynolds equation.

Heinrich and Wadhwa [1986] numerically integrated, using a Newmark finite element algorithm, the dynamic equations describing the motion of magnetic tape moving over the recording head. They considered compressibility, slip flow in the lubrication equation and flexural rigidity in the dynamic tape equation. Adams [1987] used Newton's method as a coupling scheme which applies directly to the system of equations for one-dimensional steady state foil bearing problem. The accuracy problem faced in this numerical calculation of the tape deflection is overcome by obtaining an analytical solution for the dominant component of the pressure distribution. The deflection due to the remainder of the pressure is computed numerically. He varied the viscosity of air to speed up the convergence and enhance the robustness of the solution.

Rongen [1989] presented a solution for the three-dimensional foil bearing problem, for a tape with bending stiffness and a finite width. After discretization on a grid with the finite difference method, the equations are solved simultaneously by means of a nonlinear Gauss-Seidel algorithm. Heinrich and Connolly [1992] also presented a three-dimensional finite element analysis of a self-acting foil bearing for recording head geometries. For three-dimensional calculations symmetry about the centerline of the head was used, and a zero pressure gradient condition was imposed at the center line in the lateral direction. More recently Wickert [1993] analytically studied the linear vibration of a self-pressurized foil bearing. The governing equations for the tape and recording head

are linearized about the equilibrium displacement and pressure fields, and the two resulting coupled partial differential equations with nonconstant coefficients describe the linear response.

For the case of paper webs or other porous webs correction in the Reynolds Lubrication equation is suggested in accordance with the relationship given by Yamauchi, Murakama and Imamura [1976] for the velocity of air leaking through porous webs. According to them this air leakage velocity through the porous web is proportional to the pressure difference across the web, where the constant of proportionality is the permeability coefficient of the porous media. Brundertt and Baines [1966] presented a paper on flow of air through a variety of paper sheets measured as a function of pressure difference at room temperature and observed a minimum pressure below which no flow occurred. They also described permeability as a function of sheet thickness. Later Riddiford [1969a] studied the air entrainment phenomenon between an impermeable paper web and a dryer surface of infinite width. Reducing the air gap is supposed to increase drying as the air layer is a good insulator. According to Riddiford there are three factors which decrease the air gap. If the paper is permeable, the entrained air passes through the paper. If the width of the paper is small, air flows out at the edges, and also, if either the paper or dryer is rough, air flows out spanwise at the edges. He also developed a mathematical model and solved to show the conditions under which axial variation in air gap can exist. Theoretical and experimental analysis of air films for the case of a porous web by Watanabe and Sueoka [1991] indicate a linearly decreasing

central air gap region. Otherwise, for nonporous webs this is a constant gap region. The entrance and exit region exhibit the same behavior for both the cases.

A literature review was also performed on the subject of squeeze film analyses relevant to the problem of spanwise escape of air considering finite width of the webs. Squeeze film theory suggests a non-uniform deformation of the film due to the coupled pressure distribution and squeeze flow. The results from Weinbaum, et al. [1985] show that as the height of the film decreases with time, the lateral variation of the gap between the two surfaces shows monotonic decrease from the center to the edges. Considering the finite width of a foil bearing, it is intuitive that the pressure will reduce to atmospheric towards the edges, which results in a decrease in air film thickness from the center towards the edges. Smith and Von Behren [1989], in their squeeze-film analysis of tape winding, considered a thin magnetic tape under tension, T , being wound onto a tape pack of radius R , as depicted in Figure 2.1. They developed an equation to compute the squeeze-film thickness of air entrapped between magnetic tape layers during the winding process.

Thus accurate predictions of air film gaps between a smooth roller and web must take into account the effect of porosity (if any) and sideways leakage of air due to squeeze film effects for finite width webs. This detailed literature review suggests the following approach to the numerical solution of the lubricating air-film thickness in web handling applications, considering an infinitely wide flexible web:

1. Set up the governing equations.
2. Write the finite difference forms of the two governing equations.

3. Configure the two coupled equations for simultaneous solution.
4. Impose initial conditions for the first step of the solution and boundary conditions at the two end points.
5. Define the roller surface geometry profile.
6. Develop a computer code to simultaneously solve the governing equations for an iterative solution.

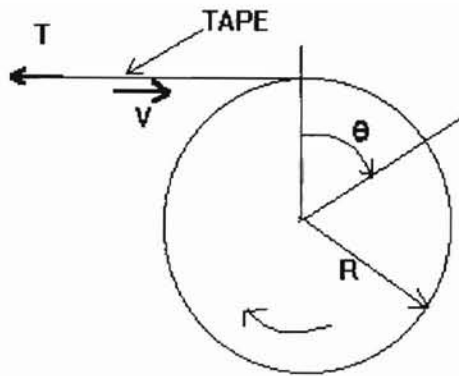


Figure 2.1 : Magnetic Tape Being Wound Onto Tape Pack Under Tension T With Tape Speed V

CHAPTER III

MATHEMATICAL FORMULATION

3.1 Problem Formulation

The problem addressed for this study is that of setting up a numerical technique to predict the air-film thickness between the roller surface and a moving web as a function of time starting from prescribed initial conditions and developing to a steady state. This will be done for the two dimensional case (infinitely wide bearing) of constant cross-web air film thickness and the effects of porosity will be added to the formulation.

To predict the lubricating air film thickness between a roller and a moving web requires the simultaneous solution of coupled equations: one, the equation of motion for a finite length of the web and second the transient lubrication equation for the air film.

3.2 Basic Equations

The partial differential equations governing both the hydrodynamic lubrication and the web motion are developed here. Almost all web handling applications involve an air film thickness which is much smaller than the radius of curvature of the lubrication film. It is therefore convenient to work in a Cartesian coordinate system. Since most web materials are also very thin, a parallel argument holds good for webs.

3.2.1 Reynolds Lubrication Equation

The hydrodynamic lubrication equation, also called the Reynolds Lubrication equation, represents a dynamic equilibrium and mass conservation for an isothermal ideal

gas, neglecting fluid inertia and assuming no variation in pressure or viscosity through the thickness of the fluid film. Consider the small element of the fluid shown in Figure 3.1.

All forces shown are per unit width into the paper.

Considering the following fact from Newton's second law

$$\Sigma F = (\text{mass}) * (\text{acceleration})$$

where,

$$\text{mass} = (\Delta x * \Delta y) * \rho, \text{ and}$$

$$\text{acceleration} = \frac{\partial V}{\partial t}$$

yields-

$$\frac{\partial \tau}{\partial y} - \frac{\partial p}{\partial x} = \rho \frac{\partial V}{\partial t} \quad (3.1)$$

and, from the Newtonian fluid constitutive relation-

$$\tau = \mu \frac{\partial V}{\partial y} \quad (3.2)$$

using equation (3.2), equation (3.1) modifies to-

$$\mu \frac{\partial^2 V}{\partial y^2} - \frac{\partial p}{\partial x} = \rho \frac{\partial V}{\partial t} \quad (3.3)$$

neglecting the fluid inertia i.e. $\rho \frac{\partial V}{\partial t} \approx 0$, yields

$$\mu \frac{\partial^2 V}{\partial y^2} - \frac{\partial p}{\partial x} = 0$$

$$\text{or, } \frac{\partial^2 V}{\partial y^2} = \frac{1}{\mu} \frac{\partial p}{\partial x} \quad (3.4)$$

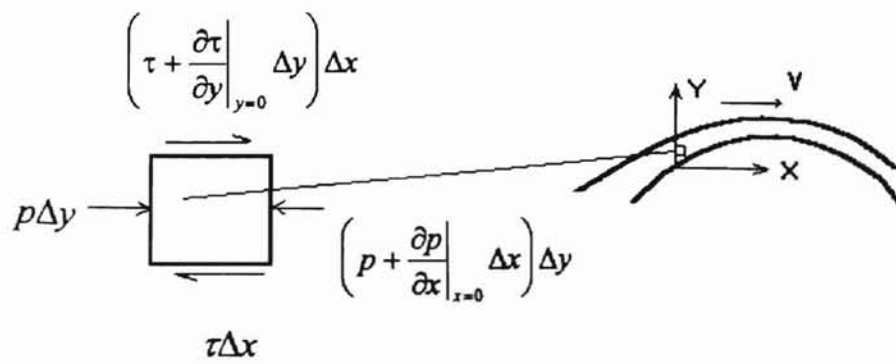


Figure 3.1 : Differential Fluid Element for Dynamic Equilibrium Analysis

integrating equation (3.4) twice gives the velocity profile

$$V = \frac{1}{2\mu} \frac{\partial \mathcal{P}}{\partial x} y^2 + C_1 y + C_2 \quad (3.5)$$

here the constants of integration C_1 and C_2 are evaluated using the boundary conditions.

Utilizing the “Slip Flow” boundary conditions, i.e., assuming that the fluid at the boundaries does not have exactly the same velocity as the boundary, but has a small amount of slip given by (Granzow and Lebeck [1984])

$$\lambda \left(\frac{\partial V}{\partial y} \right) \quad \text{where, } \lambda \text{ is the mean free path of air.}$$

At the surface of stationary roller considering slip flow,

$$V|_{y=0} = \lambda \left. \frac{\partial V}{\partial y} \right|_{y=0}$$

and, (3.6)

at the moving foil surface,

$$V|_{y=h} = V - \lambda \left. \frac{\partial V}{\partial y} \right|_{y=h}$$

These are the boundary conditions used for solving for C_1 and C_2 in equation (3.5).

Using equation (3.6) in conjunction with (3.5) yields-

$$C_1 = \frac{V - \frac{1}{2\mu} h(h + 2\lambda) \frac{\partial \mathcal{P}}{\partial x}}{(h + 2\lambda)}$$

and, (3.7)

$C_2 = \lambda C_1$. For more details refer to Appendix A

Now for a case of a nonporous web, consider the conservation of mass for the small element shown in Figure 3.2

$$Q_m - (\text{mass of element}) = Q_{out}$$

$$\Rightarrow Q_m - Q_{out} = \frac{\partial}{\partial t}(\rho h \Delta x) \quad (3.8)$$

dividing both sides of equation (3.8) by Δx and allowing $\Delta x \rightarrow 0$ yields,

$$-\frac{\partial Q}{\partial x} = \frac{\partial}{\partial t}(\rho h) \quad (3.9)$$

Now mass flow rate (per unit width) can also be obtained integrating over the velocity profile given by equation (3.5)

$$\begin{aligned} Q &= \int_0^h \rho V dy \\ &= \rho \int_0^h \left(\frac{1}{2\mu} \frac{\partial \phi}{\partial x} y^2 + C_1 y + C_2 \right) dy \\ &= \rho \left(\frac{1}{6\mu} \frac{\partial \phi}{\partial x} h^3 + \frac{C_1}{2} h^2 + C_2 h \right) \end{aligned} \quad (3.10)$$

substituting the expressions for C_1 and C_2 from equation (3.7) into equation (3.10) and rearranging, it yields-

$$Q = \rho \left(\frac{Vh}{2} - \frac{1}{12\mu} \frac{\partial \phi}{\partial x} h^3 - \frac{1}{2\mu} \frac{\partial \phi}{\partial x} h^2 \lambda \right) \quad (3.11)$$

Now using the conservation of mass equation (eq. (3.9)) and eq. (3.11) yields,

$$-\frac{\partial}{\partial x} \left[\rho \left(\frac{Vh}{2} - \frac{1}{12\mu} \frac{\partial \phi}{\partial x} h^3 - \frac{1}{2\mu} \frac{\partial \phi}{\partial x} h^2 \lambda \right) \right] = \frac{\partial}{\partial t}(\rho h) \quad (3.12)$$

For an ideal gas we have the relationship-

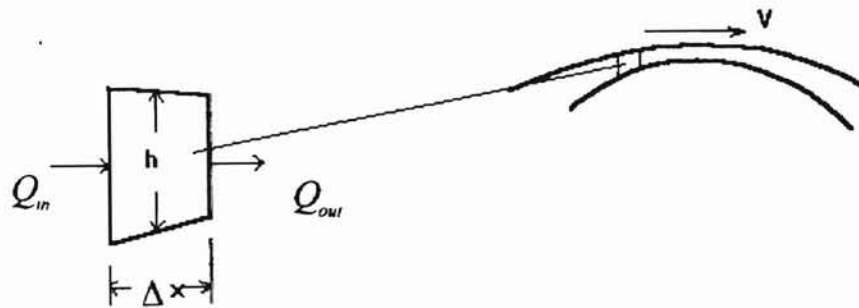


Figure 3.2 : Differential Element for Conservation of Mass Analysis for Nonporous Foil

$$\rho = \frac{P}{RT} \quad \text{where, T is the temperature and R is the gas constant} \quad (3.13)$$

assuming constant temperature, equation (3.12) can be simplified to-

$$\frac{\partial}{\partial x} \left(h^3 p \frac{\partial \phi}{\partial x} \right) + 6 \frac{\partial}{\partial x} \left(\lambda h^2 p \frac{\partial \phi}{\partial x} \right) = 6\mu V \frac{\partial}{\partial x} (ph) + 12\mu \frac{\partial}{\partial t} (ph) \quad (3.14)$$

The mean free path (λ) for an ideal gas is given by the following relationship

$$\lambda \propto \frac{1}{\rho}$$

and, therefore for an isothermal ideal gas it reduces to

$$\lambda \propto \frac{1}{p}$$

which implies that, $\lambda p = \text{constant}$

and can be replaced by the product at atmospheric conditions, i.e.,

$$\lambda p = \lambda_a p_a \quad (3.15)$$

substituting for λp from equation (3.15) into equation (3.14) yields-

$$\frac{\partial}{\partial x} \left(h^3 p \frac{\partial \phi}{\partial x} \right) + 6\lambda_a p_a \frac{\partial}{\partial x} \left(h^2 \frac{\partial \phi}{\partial x} \right) = 6\mu V \frac{\partial}{\partial x} (ph) + 12\mu \frac{\partial}{\partial t} (ph) \quad (3.16)$$

which is the **Reynolds lubrication equation** (including the slip flow and compressibility of lubricating air) for a case of a stationary roller and a moving foil.

3.2.2 Foil Equation of Motion

The foil equation of motion is a representation of Newton's second law for the foil or web. Consider the differential element of web shown in Figure 3.3. Consider the forces in the y direction-

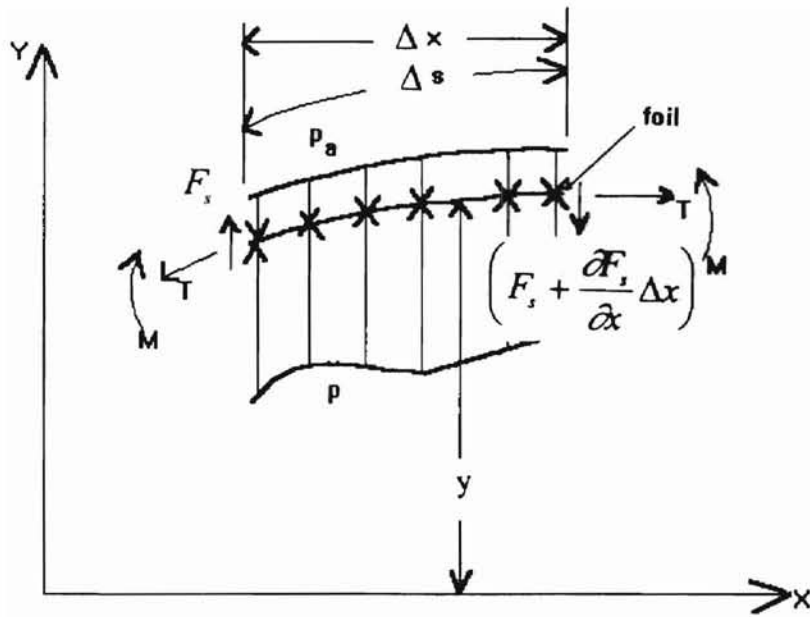


Figure 3.3 : Differential Foil Element

$$\Sigma F = w\Delta x(p - p_a) - \frac{\partial F_s}{\partial x} \Delta x + T \frac{\partial y}{\partial x} \Big|_{x+\Delta x} - T \frac{\partial y}{\partial x} \Big|_x \quad (3.17)$$

and the inertial forces in y direction will be,

$$ma = \rho(wb\Delta s) \frac{D^2 y}{Dt^2} \quad (3.18)$$

approximating $\Delta s \approx \Delta x$ for small deflections, equation (3.18) yields

$$ma = \rho(wb\Delta x) \frac{D^2 y}{Dt^2} \quad (3.19)$$

as per Newton's second law, $\Sigma F = ma$ hence equating the right hand sides of equation (3.17) and (3.19) yields,

$$w\Delta x(p - p_a) - \frac{\partial F_s}{\partial x} \Delta x + T \frac{\partial y}{\partial x} \Big|_{x+\Delta x} - T \frac{\partial y}{\partial x} \Big|_x = \rho(wb\Delta x) \frac{D^2 y}{Dt^2} \quad (3.20)$$

This can be further simplified as,

$$w(p - p_a) - \frac{\partial F_s}{\partial x} + T \frac{\partial^2 y}{\partial x^2} = \rho wb \frac{D^2 y}{Dt^2} \quad (3.21)$$

Substituting for F_s using the classical relationship between deflection and shear force:

$$F_s = EI \frac{\partial^3 y}{\partial x^3} \quad (3.22)$$

equation (3.21) yields,

$$w(p - p_a) - EI \frac{\partial^4 y}{\partial x^4} + T \frac{\partial^2 y}{\partial x^2} = \rho wb \frac{D^2 y}{Dt^2} \quad (3.23)$$

Now considering the "total derivative $D^2 y/Dt^2$,

as y is a function of both time and position x, hence

$$\frac{Dy}{Dt} = \frac{\partial y}{\partial x} \frac{\partial x}{\partial t} + \frac{\partial y}{\partial t} = \frac{\partial y}{\partial x} V + \frac{\partial y}{\partial t}$$

$$\frac{D^2 y}{Dt^2} = \frac{\partial}{\partial x} \left(\frac{Dy}{Dt} \right) \frac{\partial x}{\partial t} + \frac{\partial}{\partial t} \left(\frac{Dy}{Dt} \right)$$

$$\frac{D^2 y}{Dt^2} = \frac{\partial^2 y}{\partial x^2} V^2 + 2V \frac{\partial^2 y}{\partial x \partial t} + \frac{\partial^2 y}{\partial t^2} \quad (3.24)$$

Substituting equation (3.24) into equation (3.23) and rearranging yields the **foil equation of motion**:

$$\rho b \left(\frac{\partial^2 y}{\partial t^2} + 2V \frac{\partial^2 y}{\partial x \partial t} + V^2 \frac{\partial^2 y}{\partial x^2} \right) + \frac{EI}{w} \frac{\partial^4 y}{\partial x^4} - \frac{T}{w} \frac{\partial^2 y}{\partial x^2} = p - p_a \quad (3.25)$$

This can also be expressed in the following form:

$$\rho b \left(y_{tt} + 2Vy_{xt} + V^2 y_{xx} \right) + \frac{EI}{w} y_{xxxx} - \frac{T}{w} y_{xx} = p - p_a \quad (3.26)$$

3.3 Governing Equations

Consider a finite length of a web moving at a constant velocity V_w over a roller or support between two other support rollers, as shown is Figure 3.4 . Deflection of the web away from its equilibrium position is denoted by $y(x,t)$ and the air film thickness between the roller and web is denoted by $h(x,t)$. The pressure developed between the roller and the web is coupled to the film thickness, h , and the web tension, T , as well as other operating variables.

The system can be described using two partial differential equations which are:

1. The Web Equation of Motion (equation (3.25)):

$$\rho b \left(\frac{\partial^2 y}{\partial t^2} + 2V_w \frac{\partial^2 y}{\partial x \partial t} + V_w^2 \frac{\partial^2 y}{\partial x^2} \right) + \frac{EI}{w} \frac{\partial^4 y}{\partial x^4} - \frac{T}{w} \frac{\partial^2 y}{\partial x^2} = p - p_a$$

if we consider the foil as a plate under tension, the tension term is more dominant than

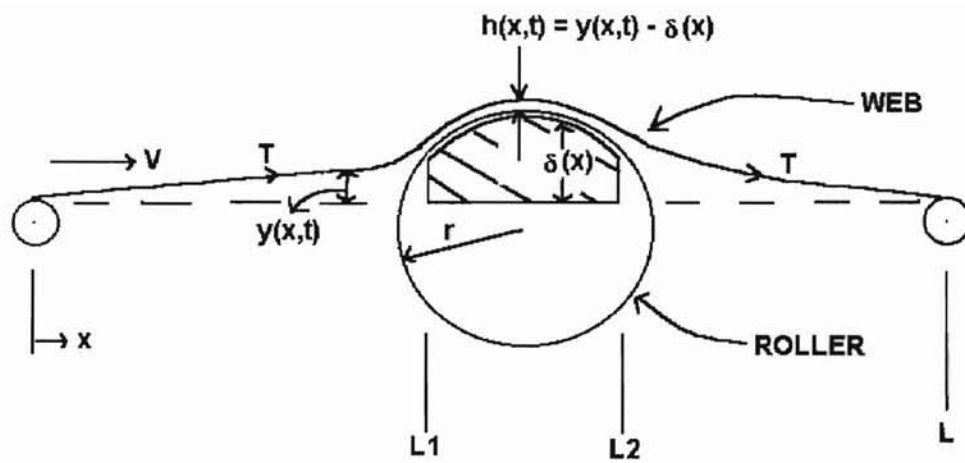


Figure 3.4 Schematic of a Web Moving Over a Roller

the stiffness of the foil. Stiffness will play a significant role if there are any elastic deformations. For a typical web conditions using order of magnitude analysis indicates that the stiffness term is very small compared to the tension term, hence can be neglected simplifying the above equation to:

$$\rho b \left(\frac{\partial^2 y}{\partial t^2} + 2V_w \frac{\partial^2 y}{\partial x \partial t} + V_w^2 \frac{\partial^2 y}{\partial x^2} \right) - \frac{T}{w} \frac{\partial^2 y}{\partial x^2} = p - p_a \quad (3.27)$$

and,

2. Reynolds Transient Lubrication Equation (equation (3.16)):

$$\frac{\partial}{\partial x} \left(h^3 p \frac{\partial p}{\partial x} \right) + 6\lambda_a p_a \frac{\partial}{\partial x} \left(h^2 \frac{\partial p}{\partial x} \right) = 6\mu V_w \frac{\partial}{\partial x} (ph) + 12\mu \frac{\partial}{\partial t} (ph) \quad (3.28)$$

The two governing equations are coupled through the pressure (p) and through the following relationship between the film thickness (h) and the foil displacement (y):

$$h(x, t) = y(x, t) - \delta(x) \quad (3.29)$$

where, $\delta(x)$ is a function describing the roller surface geometry.

The Reynolds Lubrication equation needs to be modified for the case of a rotating roller and porous webs (eg. paper). If V_R , V_w and V_i are the roller surface velocity, web velocity and velocity of air through (in the direction perpendicular to the web velocity) the porous web respectively, then the Reynolds Lubrication equation modifies to (details are provided in Appendix B)-

$$\frac{\partial}{\partial x} \left(h^3 p \frac{\partial p}{\partial x} \right) + 6\lambda_a p_a \frac{\partial}{\partial x} \left(h^2 \frac{\partial p}{\partial x} \right) = 6\mu(V_R + V_w) \frac{\partial}{\partial x} (ph) + 12\mu \frac{\partial}{\partial t} (ph) + 12\mu p V_i$$

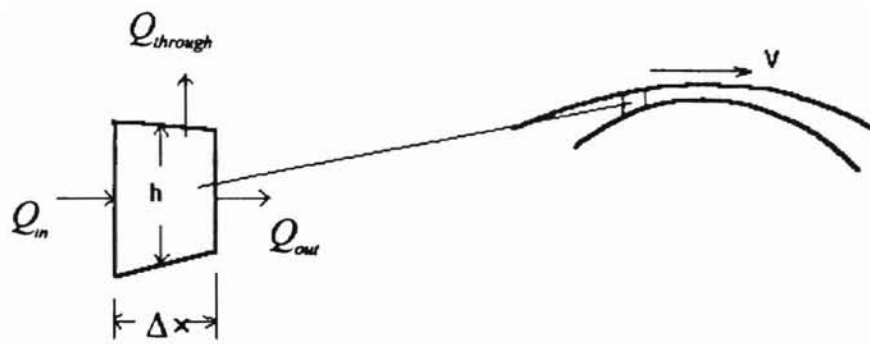


Figure 3.5 Differential Element for Conservation of Mass Analysis for Porous Foil

but, the velocity of air through the porous web, as suggested by Murakama and Imamura [1976] is-

$$V_i \propto (p - p_a)$$

$$\Rightarrow V_i = K(p - p_a)$$

thus the Reynolds Lubrication equation takes the following form,

$$\frac{\partial}{\partial x} \left(h^3 p \frac{\partial p}{\partial x} \right) + 6\lambda_a p_a \frac{\partial}{\partial x} \left(h^2 \frac{\partial p}{\partial x} \right) = 6\mu(V_R + V_w) \frac{\partial}{\partial x} (ph) + 12\mu \frac{\partial}{\partial t} (ph) + 12\mu K p (p - p_a)$$

or

$$\frac{\partial}{\partial x} \left(h^3 p \frac{\partial p}{\partial x} \right) + 6\lambda_a p_a \frac{\partial}{\partial x} \left(h^2 \frac{\partial p}{\partial x} \right) = 6\mu(V_R + V_w) \frac{\partial}{\partial x} (ph) + 12\mu \frac{\partial}{\partial t} (ph) + 12 \frac{k}{b} p (p - p_a)$$

where,

k = permeability coefficient of porous web (m^2)

K = permeability of porous web $\left(\frac{m^3/\text{sec.}}{m^2 - Pa} \right)$

b = thickness of the web (m), and

$(p - p_a)$ = pressure drop across the porous web.

3.4 Boundary Conditions

Referring to Figure 3.4, the boundary conditions for the problem here are taken to be-

$$y(L_1, t) = y(L_1, 0) = \text{constant},$$

$$y(L_2, t) = y(L_2, 0) = \text{constant},$$

$$y_x(L_1, t) = y_x(L_1, 0) = \text{constant, and}$$

$$y_x(L_2, t) = y_x(L_2, 0) = \text{constant}$$

The y 's at two ends L_1 and L_2 are calculated directly based upon roller geometry.

The pressure is taken to be ambient at the ends of the roller,

$$p(L_1, t) = p(L_2, t) = p_a .$$

3.5 Initial Conditions

Referring to Figure 3.6 the initial conditions for air film gap and pressure for the domain within the tangency points are-

$$h = h_o = 0.643R \left(6\mu \frac{(V_R + V_w)}{T} \right)^{2/3} = \text{constant, and}$$

$$p = p_o = p_a + \frac{T/w}{R} = \text{constant.}$$

For the region outside the tangency point the displacement is taken to be linear and pressure to be atmospheric.

3.6 Tangency Point Location

Initial conditions described above are for the regions within the tangency points and outside the tangency points. Therefore the determination of the tangency points i.e. the locations on the roller surface where the web is tangent to the roller is required. Referring to Figure 3.6 one can geometrically obtain the expressions for X_0 and Y_0 i.e.

$$X_0 = 0.5*L - (R + h_o)*\text{Sin}\theta$$

$$Y_0 = (\delta_{\max} - R) + (R + h_o)*\text{Cos}\theta$$

where,

X_0 is the X-axis coordinate for the tangent point,

Y_0 is the Y-axis coordinate for the tangent point, and

θ is the included angle between the web and the reference line.

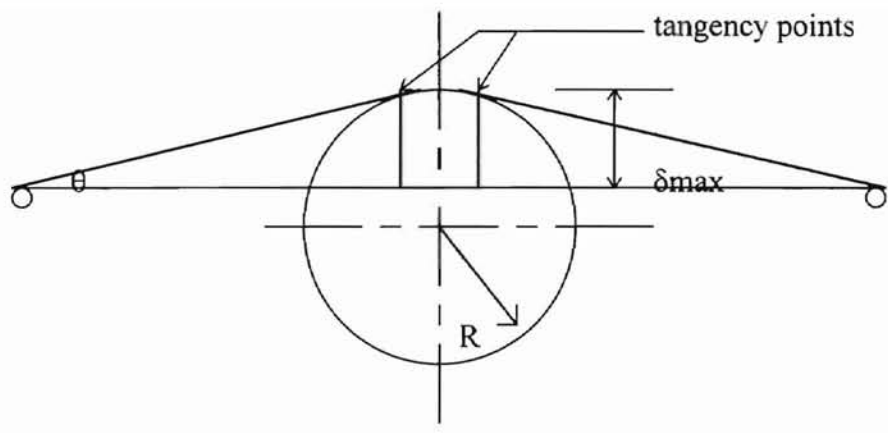


Figure 3.6 : Schematic Indicating the Tangency Points for Initial Conditions

CHAPTER IV

FINITE DIFFERENCE SOLUTION APPROACH

As discussed in CHAPTER III the system of web moving over a stationary or rotating roller can be described using two partial differential equations, which are-

1. The Web Motion Equation

$$\rho b \left(\frac{\partial^2 y}{\partial t^2} + 2V_w \frac{\partial^2 y}{\partial x \partial t} + V_w^2 \frac{\partial^2 y}{\partial x^2} \right) - \frac{T}{w} \frac{\partial^2 y}{\partial x^2} = p - p_a$$

which can also be written in the following form-

$$\rho b \left(y_{tt} + 2V_w y_{xt} + V_w^2 y_{xx} \right) - \frac{T}{w} y_{xx} = p - p_a \quad (4.1)$$

and,

2. Reynolds Lubrication Equation

$$\frac{\partial}{\partial x} \left(h^3 p \frac{\partial p}{\partial x} \right) + 6\lambda_a p_a \frac{\partial}{\partial x} \left(h^2 \frac{\partial p}{\partial x} \right) = 6\mu(V_R + V_w) \frac{\partial}{\partial x} (ph) + 12\mu \frac{\partial}{\partial t} (ph) + 12\mu Kp(p - p_a)$$

which can be expanded and expressed in the following form-

$$\begin{aligned} & \left(h^3 p p_{xx} + h^3 p_x^2 + 3h^2 p p_x h_x \right) + 6\lambda_a p_a \left(h^2 p_{xx} + 2h p_x h_x \right) = \left[12\mu (p h_t + h p_t) \right. \\ & \left. + 6(V_R + V_w) \mu (p_x h + h_x p) + 12\mu Kp(p - p_a) \right] \end{aligned} \quad (4.2)$$

The two governing equations are coupled through the pressure, p and the following relationship between the air film thickness, h(x,t) between the roller and web and the web displacement, y(x,t) with respect to the equilibrium position:

$$h(x,t) = y(x,t) - \delta(x) \quad (4.3)$$

where, $\delta(x)$ is a function describing the roller surface geometry.

The system of equations (4.1)-(4.3) is solved by substituting the proper finite difference operators for the derivatives and thus solving the resultant finite difference equations simultaneously using the boundary and initial conditions discussed in section 3.4 and 3.5 respectively.

The coupling of equations (4.1) and (4.2) through equation (4.3) is accomplished by solving the finite difference equation corresponding to equation (4.2) for pressure, p , at a given time step, using the existing solution for air film gap, $h(x,t)$, from equation (4.1), and then solving the difference equation corresponding to equation (4.1) for new values of web displacement, $y(x,t)$, using the latest values of pressure, p , from equation (4.2). This is performed iteratively until steady state is reached.

The finite difference operators used for solving equations (4.1) and (4.2) are-

$$y_{xx} = \frac{\partial^2 y}{\partial x^2} = (y_{i+1}^{n+1} - 2y_i^{n+1} + y_{i-1}^{n+1})/\Delta x^2$$

$$y_{tt} = \frac{\partial^2 y}{\partial t^2} = (y_i^{n+1} - 2y_i^n + y_i^{n-1})/\Delta t^2$$

$$y_{xt} = \frac{\partial^2 y}{\partial x \partial t} = (y_{i+1}^{n+1} - y_{i+1}^{n-1} - y_{i-1}^{n+1} + y_{i-1}^{n-1})/4\Delta x \Delta t$$

$$p_x = \frac{\partial p}{\partial x} = (p_{i+1}^{n+1} - p_{i-1}^{n+1})/2\Delta x$$

$$p_t = \frac{\partial p}{\partial t} = (p_i^{n+1} - p_i^n)/\Delta t$$

$$p_{xx} = \frac{\partial^2 p}{\partial x^2} = (p_{i-1}^{n+1} - 2p_i^{n+1} + p_{i+1}^{n+1})/\Delta x^2$$

$$h_x = \frac{\partial h}{\partial x} = (h_{i+1}^{n+1} - h_{i-1}^{n+1})/2\Delta x$$

$$h_t = \frac{\partial h}{\partial t} = (h_i^{n+1} - h_i^n)/\Delta t$$

substituting the finite difference operators in equation (4.1) reduces the web motion equation to the form-

$$B_1 y_{i-1}^{n+1} + D_1 y_i^{n+1} + A_1 y_{i+1}^{n+1} = E_1 \quad (4.4)$$

where, B_1, D_1, A_1 are constants containing coefficients from equation (4.1) and E_1 contains the values of foil displacement, $y(x,t)$ at time step n and $(n-1)$ and, pressure, p at time step n (for more details see Appendix C).

Similarly substituting the finite difference operators in equation (4.2) reduces the Reynolds Lubrication equation to the form-

$$B_2 p_{i-1}^{n+1} + D_2 p_i^{n+1} + A_2 p_{i+1}^{n+1} = E_2 \quad (4.5)$$

where, B_2, D_2, A_2 and E_2 contain the values of pressure, p , at time step, n , and values of air film gap, $h(x,t)$, at time step, n , and $(n+1)$ obtained solving equation (4.4) (for more details see Appendix C). The finite difference form of the Reynolds Lubrication equation will be nonlinear. This is inconvenient to solve, if the above finite difference operators are used. The equation is linearized as given by Stahl et al. [1974] using an approximation at the old time step n instead of the new time step $(n+1)$ in those terms involving products of p and its derivatives. To understand how this is done, consider the first term in the Reynolds lubrication equation. The result after carrying out the differentiation is $(h^3 pp_{xx} + h^3 p_x^2 + 3h^2 pp_x h_x)$. If p_i^n is used for p instead of p_i^{n+1} and a

difference approximation involving n instead of $n + 1$ is used for p_x , then the result is linear in those values of p at time step $n + 1$

A grid of mesh Δx is chosen and the time step Δt is chosen small enough to ascertain the numerical stability of the solution. To determine a suitable value of Δt for a chosen Δx , a “Steady State” solution was calculated using a relatively large value for Δt . Next, the solution was continued for smaller Δt . If the solution obtained after a few iterations changed substantially, the solution was continued for smaller Δt . For stability in this numerical technique a time step of 5×10^{-7} second or smaller has to be used. For larger time steps it was found that the numerical solution becomes unstable. The time period or the number of iterations from transient to the steady state solution was approximated to be 125% of the ratio of the length of web wound around the roller to the web-roller velocity. As the finite difference form of the two governing equations reduce to Tri-Diagonal Matrices, the solution is sought using the Tri-Diagonal Matrix Algorithm. This applies Gauss’ elimination method with the boundary and initial conditions discussed in section 3.4 and 3.5 respectively. The Tri-Diagonal Matrix Algorithm is used as described by Lilley [1992].

CHAPTER V

RESULTS

Numerical computations were performed to study the transient behavior of the web moving over a smooth roller and to predict the distribution of lubricating air film thickness between moving nonporous or porous webs and a smooth rotating or stationary roller. In these two-dimensional computations, the infinitely wide web was moving over a roller in the longitudinal direction with two distant end supports as shown in Figure 3.4

A FORTRAN code is developed to solve the finite difference forms of the governing equations presented in CHAPTER IV. The code simultaneously solves the two finite difference equations yielding the spacing and pressure distribution between the moving web and the roller (which can be either stationary or rotating) as a function of both time and distance along the roller. This transient solution finally converges to the steady state solution.

The roller profile is first defined with the distance of the roller surface from a reference line joining the two end supports. All distances in the direction perpendicular to the motion of the web are measured with respect to this line (refer to Figure 3.4) joining the two end supports. The air film thickness above the roller surface is obtained by subtracting the roller profile from the displacement of the web with respect to the reference line. The foil is assumed to be infinitely wide with zero bending stiffness but with mass.

TABLE 1

Sample simulation parameters for film thickness computation for web-roller interface

Web parameters :

$\rho_b = 0.0610 \text{ kg/m}^2$, web mass per unit area

$T/w = 262 \text{ N/m}$, web tension per unit width (of the web)

$V_w = 5.08 \text{ m/s}$, web velocity

Lubrication parameters :

$\mu = 1.81 \times 10^{-5} \text{ Pa} \cdot \text{s}$, dynamic viscosity of air

$p_a = 84.1 \text{ kPa}$, ambient pressure

$\lambda_a = 0.0635 \text{ } \mu\text{m}$, mean free path length of air at ambient pressure

Roller and web geometry (see Figure 3.4) :

$L = 0.85 \text{ m}$, distance between the two end supports

$L_1 = 0.35 \text{ m}$, location of left reference point on the roller

$L_2 = 0.50 \text{ m}$, location of right reference point on the roller

$R = 0.20 \text{ m}$, roller radius

Finite difference parameters :

$\Delta t = 5 \times 10^{-7} \text{ s}$, time step for numerical solution

$\Delta x = 1.23 \times 10^{-3} \text{ m}$, grid size for numerical solution

5.1 Results for Nonporous (infinitely wide) Webs

Initial computations with a roller of 40 mm diameter were performed to allow comparison with results in the magnetic recording tape literature. Transient profiles were obtained for a web moving over a stationary roller with web tension, $T=1.58 \text{ lb/in}$ (277 N/m)* and web velocity, $V=500 \text{ ft/min}$ (2.54 m/s). The two results are in very close agreement. According to the results given by Stahl, et al. [1974] the steady state spacing neglecting slip flow and stiffness is calculated to be $50.4 \mu\text{in}$ ($1.26 \mu\text{m}$) whereas it is about $48.2 \mu\text{in}$ ($1.224 \mu\text{m}$) using the code developed for this study. The transient air film thickness profiles are shown in Figure 5.1 and the pressure profiles in Figure 5.2 for this combination of tension and velocity. The solution for this case reaches steady state after about 6 milliseconds. The steady state time depends upon the length of the roller around which the web is wound and the combined speed of the web and roller surface. The angle of wrap for the computations presented in this chapter is approximately 20° . The distance along the roller is non-dimensionalized considering the entire domain, i.e. distance between L_1 and L_2 (refer Figure 3.4), to be of unit length.

The steady state air film thickness for the central constant gap region assuming no slip condition at the foil and roller surface for the above combination of tension and velocity is about $48.2 \mu\text{in}$ ($1.224 \mu\text{m}$), approximately $0.083 \mu\text{m}$ less than the classical air film thickness given by the Knox-Sweeney equation (equation 1.7). This difference of approximately two percent from the classical solution is insignificant from the practical viewpoint, because experimental results generally introduce substantially greater error.

* The figures within parentheses (on graphs also) are in S.I. Units. Velocity (V) in m/s and Tension (T) in N/m .

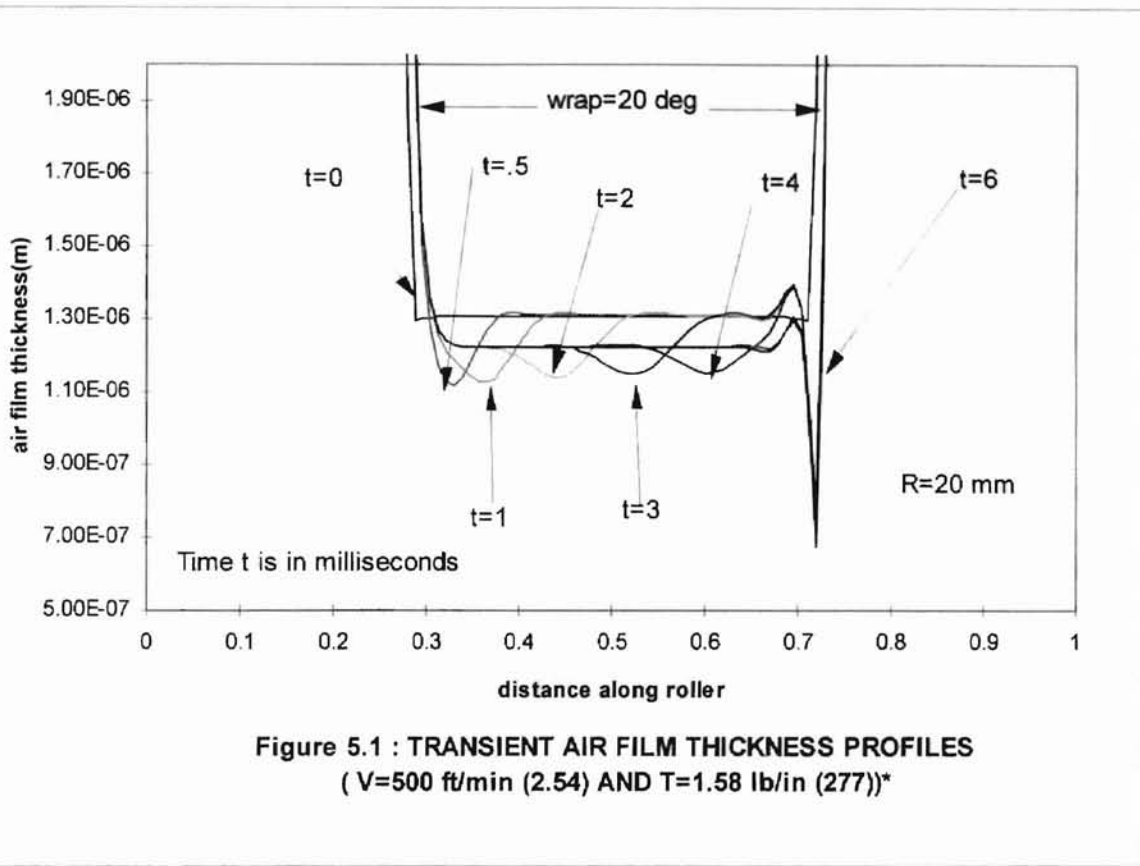


Figure 5.1 : TRANSIENT AIR FILM THICKNESS PROFILES
 (V=500 ft/min (2.54) AND T=1.58 lb/in (277))*

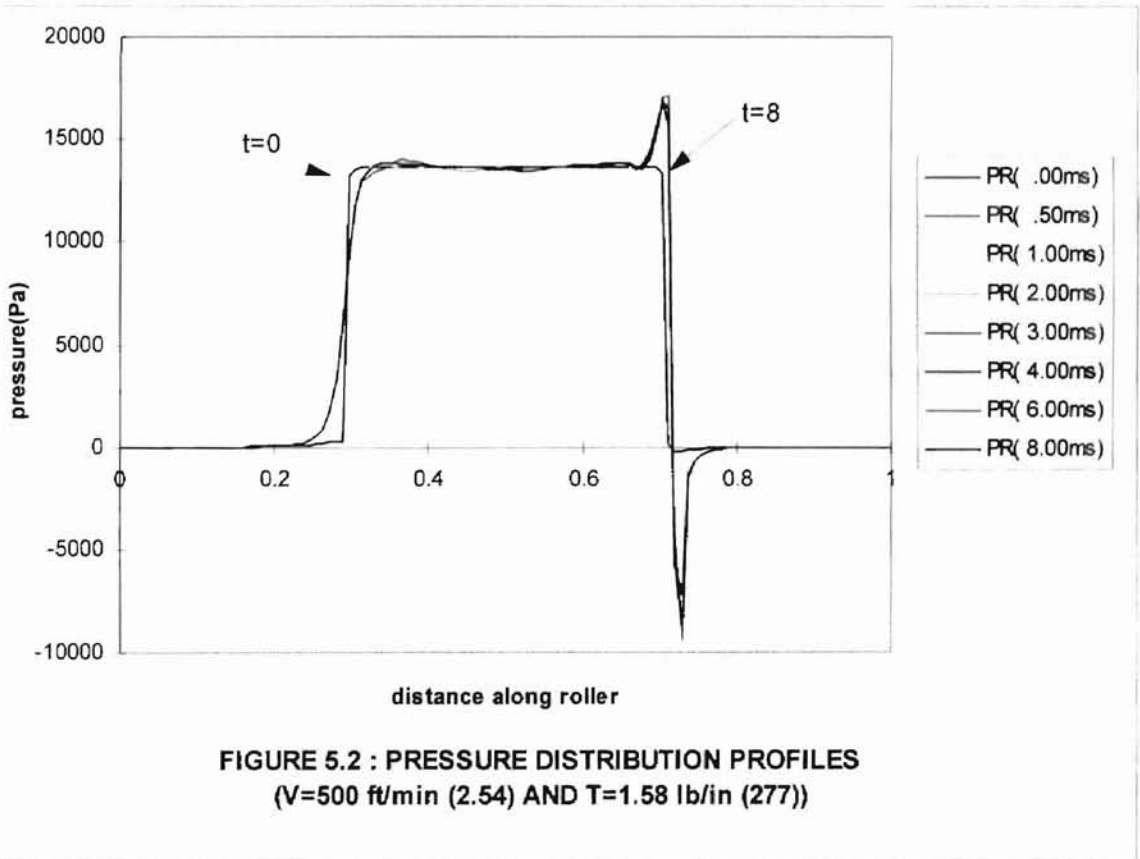


FIGURE 5.2 : PRESSURE DISTRIBUTION PROFILES
 (V=500 ft/min (2.54) AND T=1.58 lb/in (277))

Considering slip flow tends to reduce the air film gap further, as shown in Figure 5.3. The effect of slip flow decreases at the higher web velocities as shown in Figure 5.4, i.e., the air film thickness remains almost the same with or without considering slip flow at higher velocities. Moreover for high speed web handling applications the air-film thickness is of the order of 10^{-5} or 10^{-4} m which is very large compared to the mean free path of air which is of the order of 10^{-8} m. Thus neglecting slip flow for such an application is a valid assumption. The results also show the characteristic exponential decrease in air film thickness for the entrance region and sinusoidal behavior at the exit region as given by foil bearing theory. A better understanding of foil bearing predictions can be grasped from Figure 5.5 which shows the combined steady state air film thickness profile and pressure profile. In the entrance region (refer to Figure 1.3) pressure increases from ambient to the film pressure, P and a decrease in air gap occurs smoothly and is exponential in form. Next comes the central constant gap region. The air film gap, h_0 and pressure, P remain constant for this region. The last region is the exit region where pressure decreases from P to ambient pressure while the gap increases from h_0 to infinity. From the Reynolds equation it is obvious that a negative pressure gradient can exist only if the air gap at the exit is less than h_0 , which is incompatible with an increasing gap. The increase in gap is therefore preceded by a region where the air film gap is less than h_0 in which pressure decreases to below ambient followed by a region of increasing gap and increasing pressure.

After a sound initial comparison with the results in the magnetic recording tape literature the roller geometry was modified to study the foil bearing predictions for a

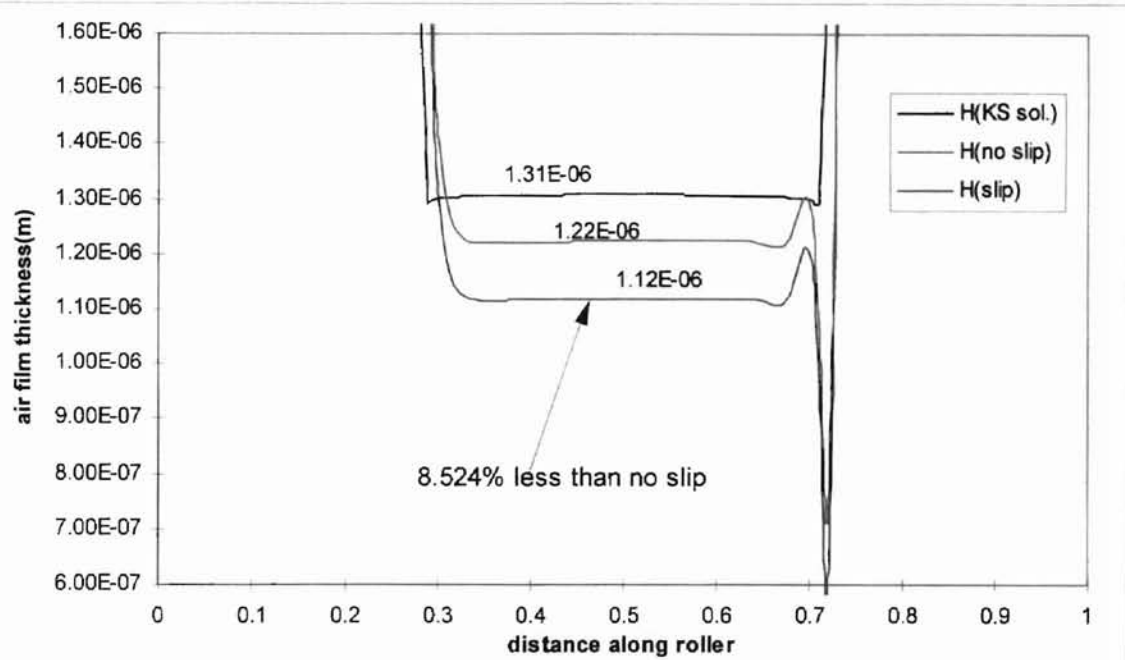


FIGURE 5.3 : COMPARISON OF AIR FILM THICKNESS WITH AND WITHOUT SLIP FLOW FOR LOW WEB VELOCITY (V=500 ft/min (2.54) AND T=1.58 lb/in (277))

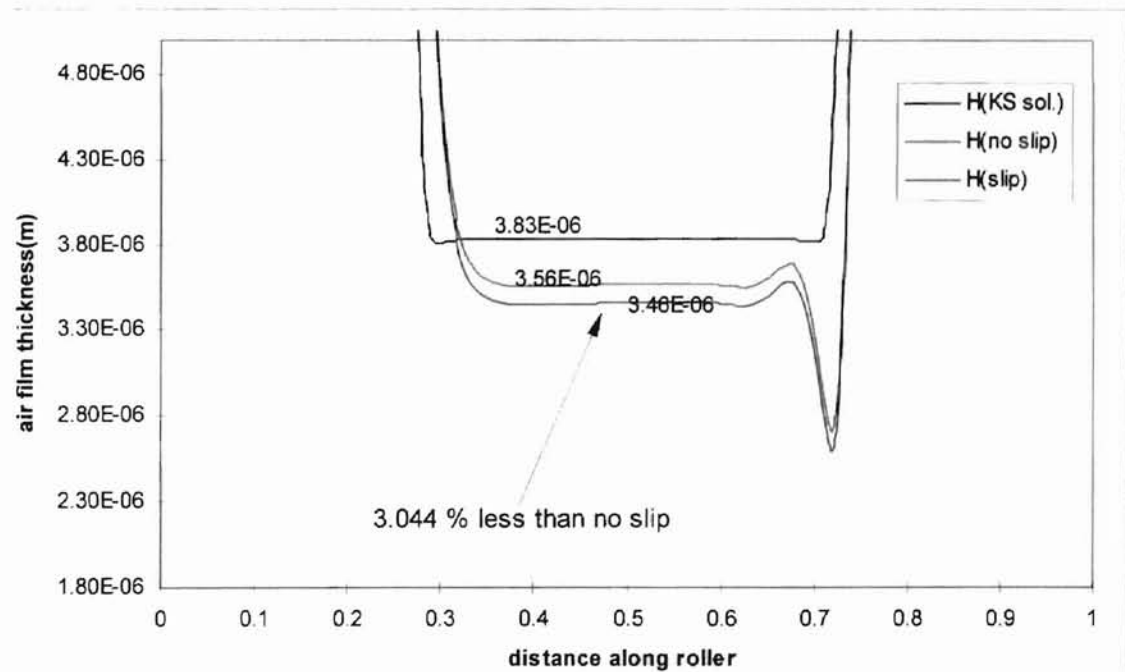
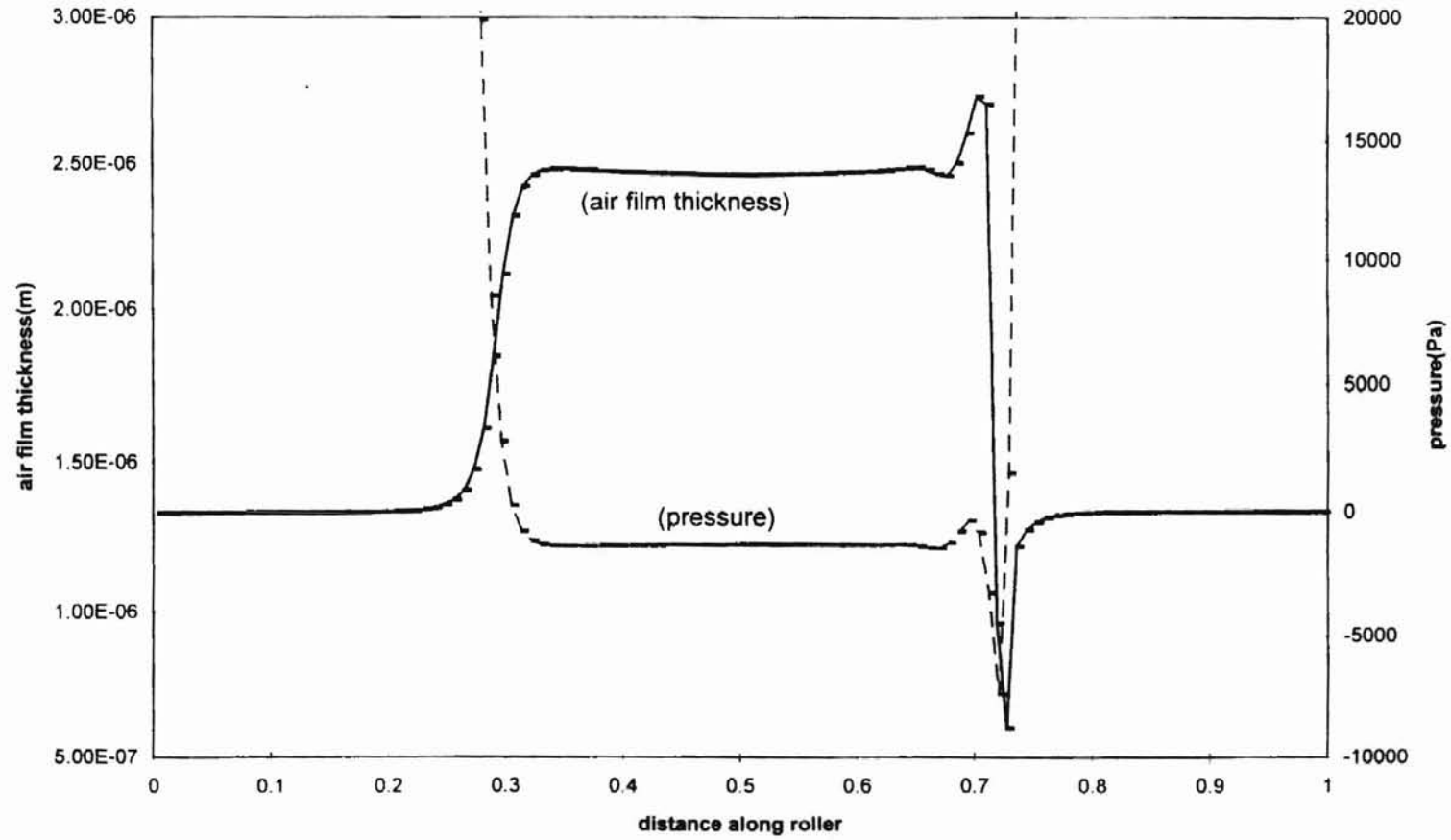


FIGURE 5.4 : COMPARISON OF AIR FILM THICKNESS WITH AND WITHOUT SLIP FLOW FOR HIGH WEB VELOCITY (V=2500 ft/min (12.7) AND T=1.58 lb/in (277))



**Figure 5.5 : COMBINED AIR FILM THICKNESS PROFIL AND PRESSURE DISTRIBUTION PROFILE
(V=500 ft/min (2.54) AND T=1.58 lb/in (277))**

bigger roller of radius 20 cm. Figure 5.6 presents transient air film thickness profiles for a case with web tension, $T=1.5$ lb/in (263 N/m) and velocity, $V=1000$ ft/min (5.08 m/s). For this case the transient period is about 30 milliseconds and the steady state air film thickness is approximately 829.92 μ in (21.08 μ m). Figure 5.7 presents the transient air film thickness profile for a case with web tension, $T=1.5$ lb/in (263 N/m) and velocity, $V=3000$ ft/min (15.24 m/s). For this case the transient period is about 10 milliseconds and the steady state air film thickness is approximately 1736.22 μ in (44.1 μ m). Thus the transient period decreases as the velocity of the web increases, other parameters remaining the same. Figures 5.8 and 5.9 illustrate the effects of varying tension and varying web velocity, respectively, on the steady state air film thickness. Increasing tension tends to reduce the air film thickness but increasing velocity increases the air film thickness by entrapping more between the moving web and the support roller. An increase in the length of the constant gap central region can be seen (Figure 5.8) with the increase in web tension increasing the area of contact between the web and the support roller. The reduction in air film thickness due to slip can now be understood, because of the slip flow the air film adjacent to the web is at lower velocity than the web itself hence the steady state air film thickness is lower compared to the no slip flow condition. However it is already seen that the effect of slip flow at higher velocities, with their greater film thickness, is negligible.

Next the effect of web mass on the steady state air film thickness is considered. Figure 5.10 shows the steady state air film thickness profile for cases of varying web mass per unit area at velocity, $V=1000$ ft/min (5.08 m/s) and tension, $T=1.5$ lb/in (263

N/m). The profiles for different web mass virtually coincide, indicating a very small effect of web mass at this low velocity. A close look at the central region profile (Figure 5.11) indicates very small increases in air film thickness as the mass increases, only about 1.0% for a 394% increase in web mass. Figures 5.12 and 5.13 display the results for a higher web velocity, $V=3000$ ft/min (15.24 m/s) with the same tension. For this case the increase in steady state air film thickness is about 11.5% for the same increase in web mass, indicating the effect of mass at higher web velocities. Thus there is an implied reduction in web-roller traction due to increase in web mass at the same operating conditions. These results are extended to the case of a web moving over a rotating roller. The pattern of air film thickness and pressure profile remains the same, with the effect of the rotating roller being a net increase in velocity and thereby an increase in air film thickness as compared to the case of the stationary roller shown in Figure 5.14. From the results of the two different roller radii presented it can be concluded that for the larger radius, more air is entrapped between the support roller and the moving web .

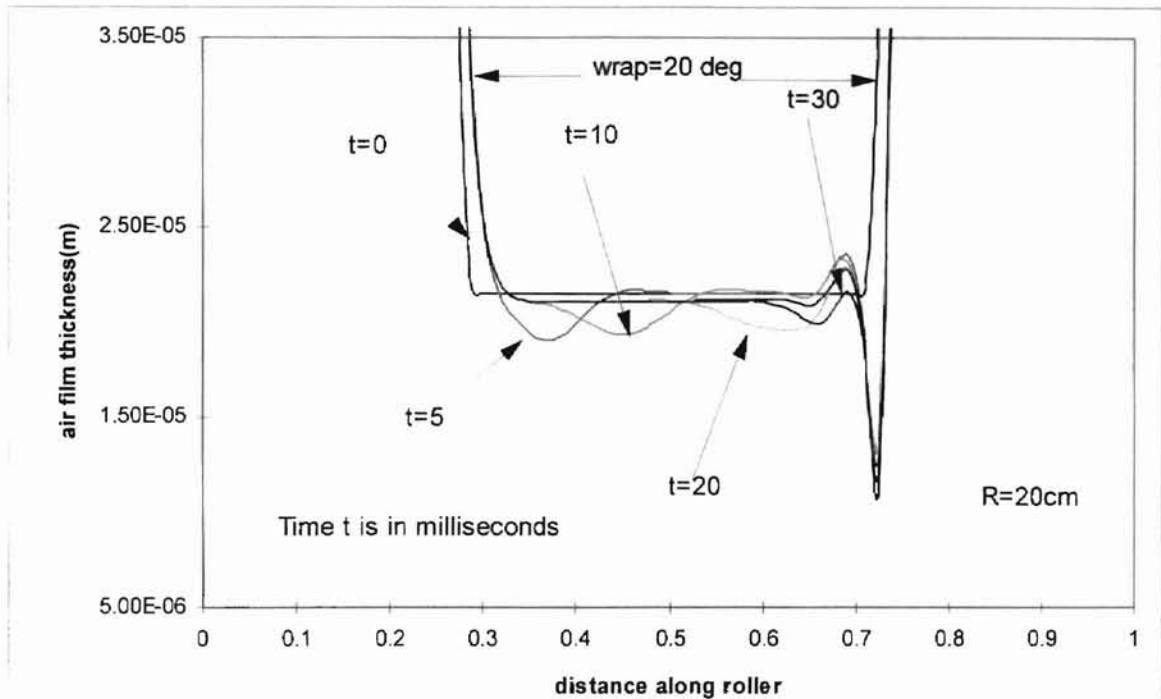


**FIGURE 5.6 : TRANSIENT AIR FILM THICKNESS PROFILES
($V=1000$ ft/min (5.08) AND $T=1.5$ lb/in (263))**

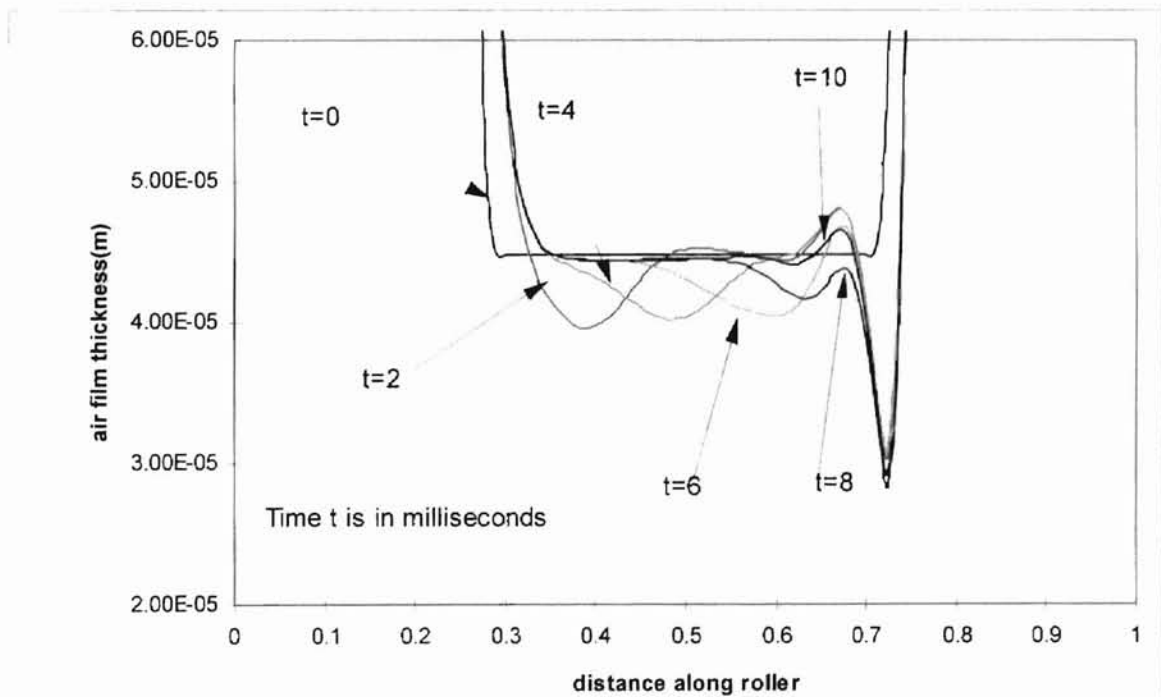


**FIGURE 5.7 : TRANSIENT AIR FILM THICKNESS PROFILES
($V=3000$ ft/min (15.24) AND $T=1.5$ lb/in (263))**

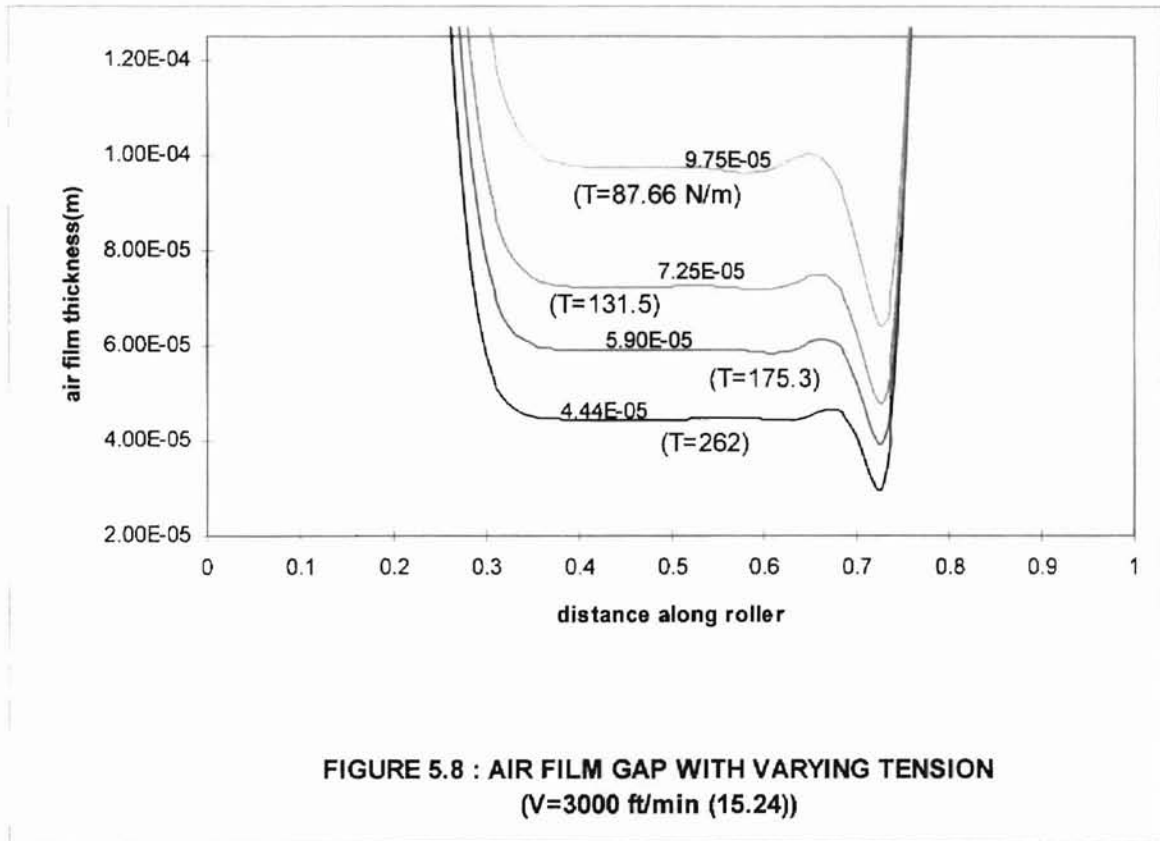


FIGURE 5.8 : AIR FILM GAP WITH VARYING TENSION
(V=3000 ft/min (15.24))

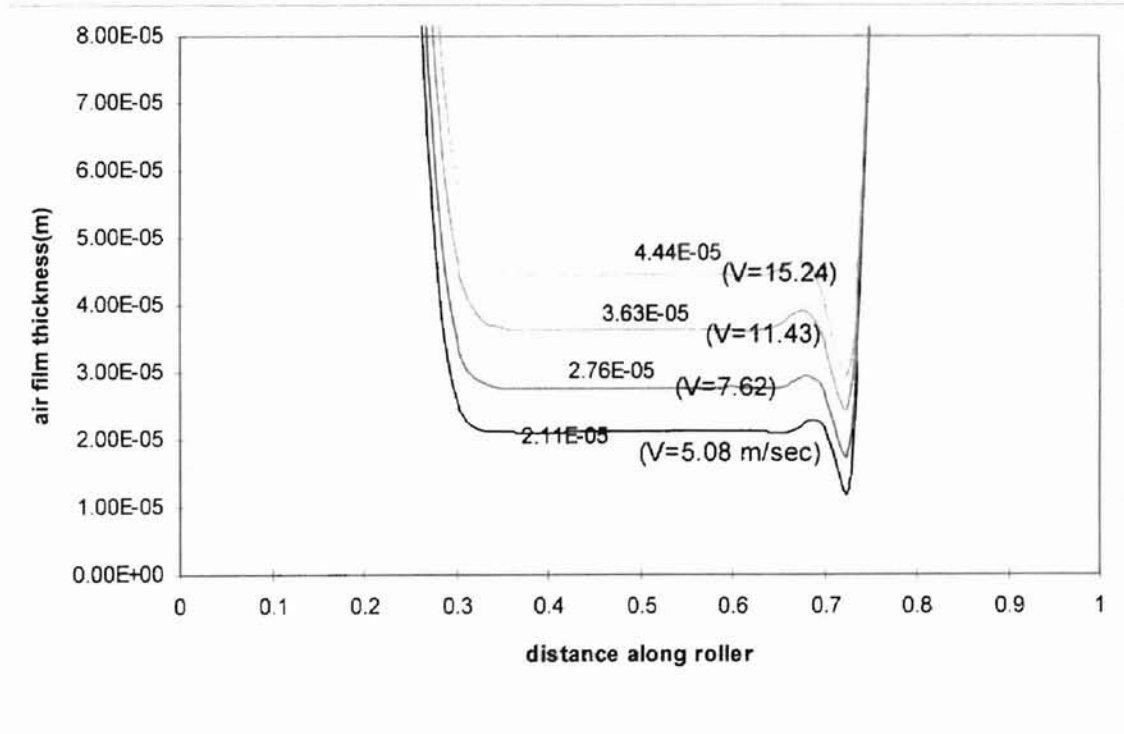
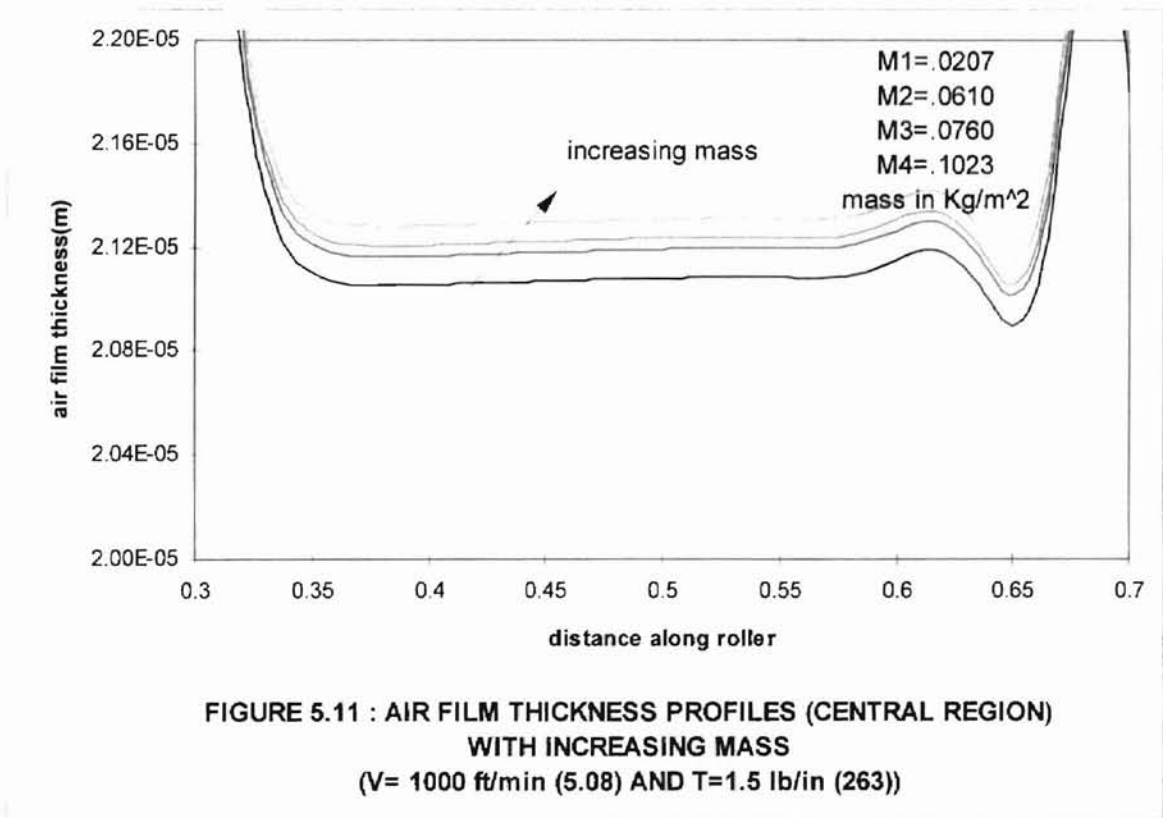
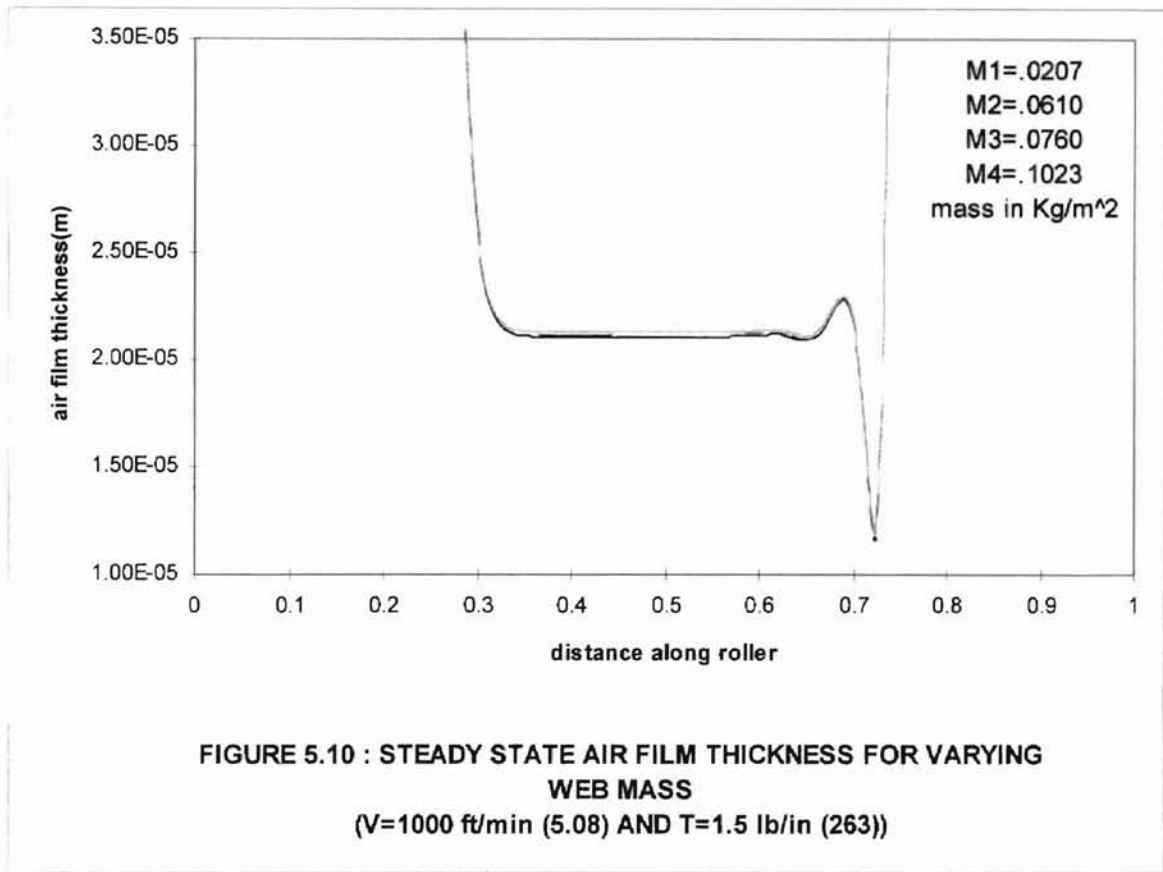
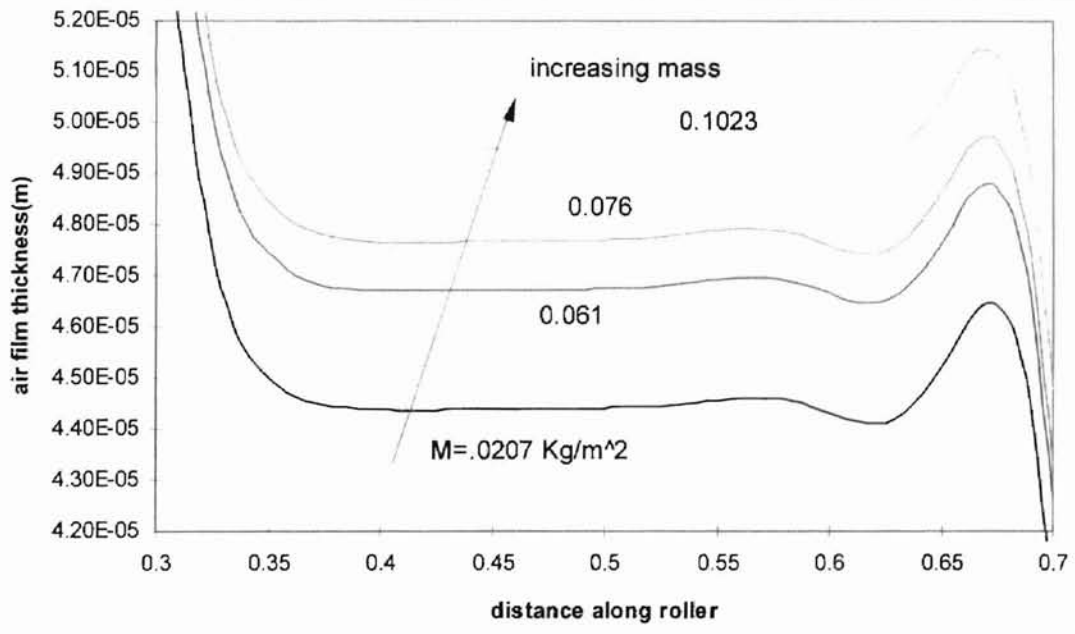
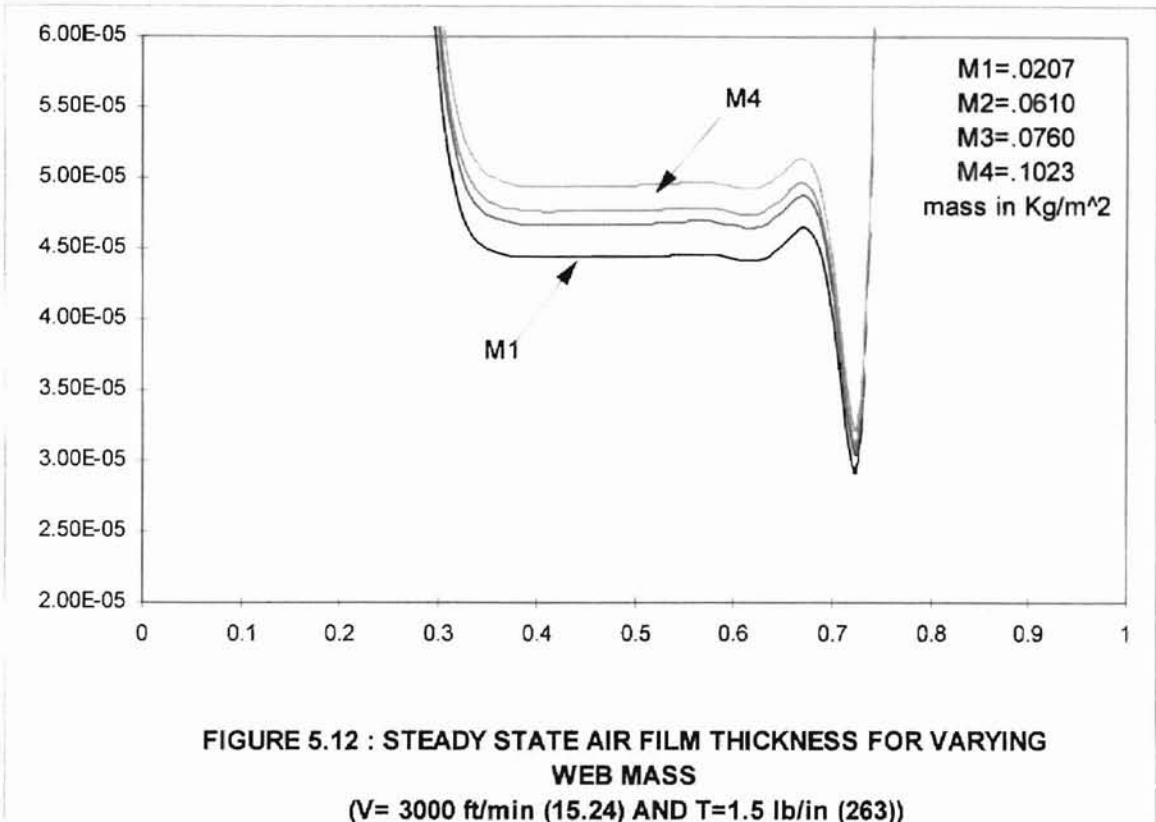


FIGURE 5.9 : AIR FILM THICKNESS WITH VARYING WEB VELOCITY
(T=1.5 lb/in (263))





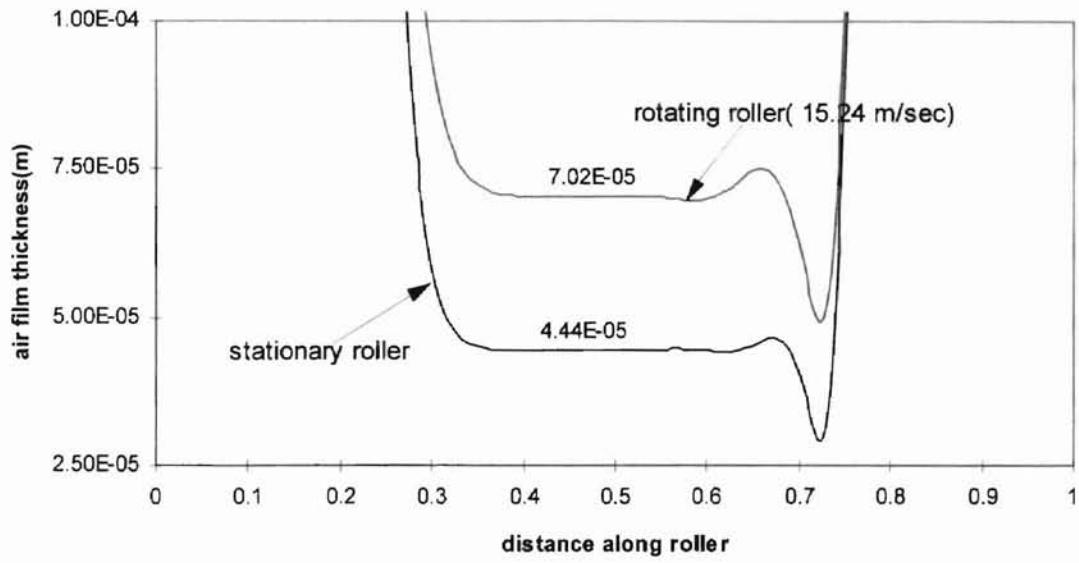


FIGURE 5.14 : COMPARISON OF STEADY STATE AIR FILM GAP FOR STATIONARY AND ROTATING ROLLER (V=3000 ft/min (15.24) AND T=1.5 lb/in (263))

5.2 Results for Porous Webs

Results for the case of porous webs are presented for roller radius 30.48 cm to allow comparison with the results presented in the study by Ducotey and Good [1996]. Results show the characteristic linearly decreasing air film thickness for the central region around the circumference of the roller, and entrance and exit region behaviors similar to those of nonporous webs. This nearly linear decrease in the air film gap for the central region is a function of web-roller velocity, web tension and web permeability. The decrease in the air film gap is not exactly linear but the slope of the decreasing profile increases slightly along the roller. As the radius of curvature along the roller decreases the air film pressure increases, thus decreasing the air gap. However, the increase in pressure in the decreasing air gap region is not significant for typical web handling conditions and can be approximated as a constant pressure region. Ducotey and Good [1996] developed an approximate equation for predicting the air film height between a permeable web and roller in the central gap region, which can be expressed as-

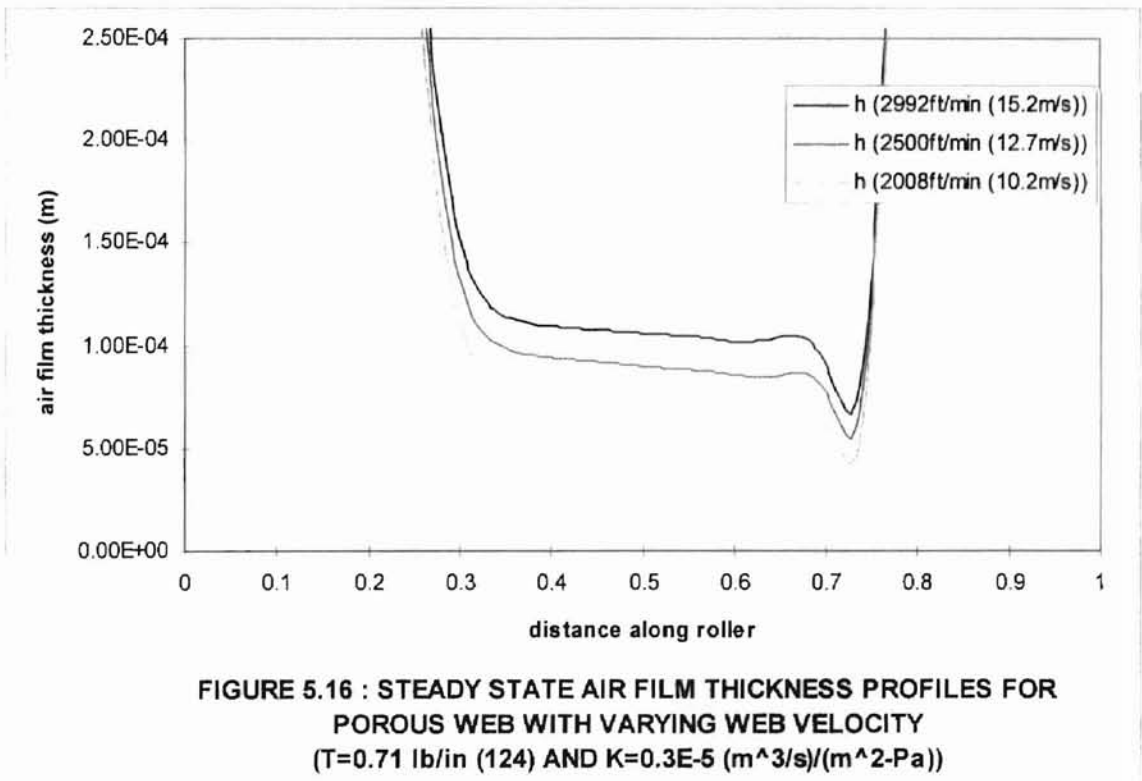
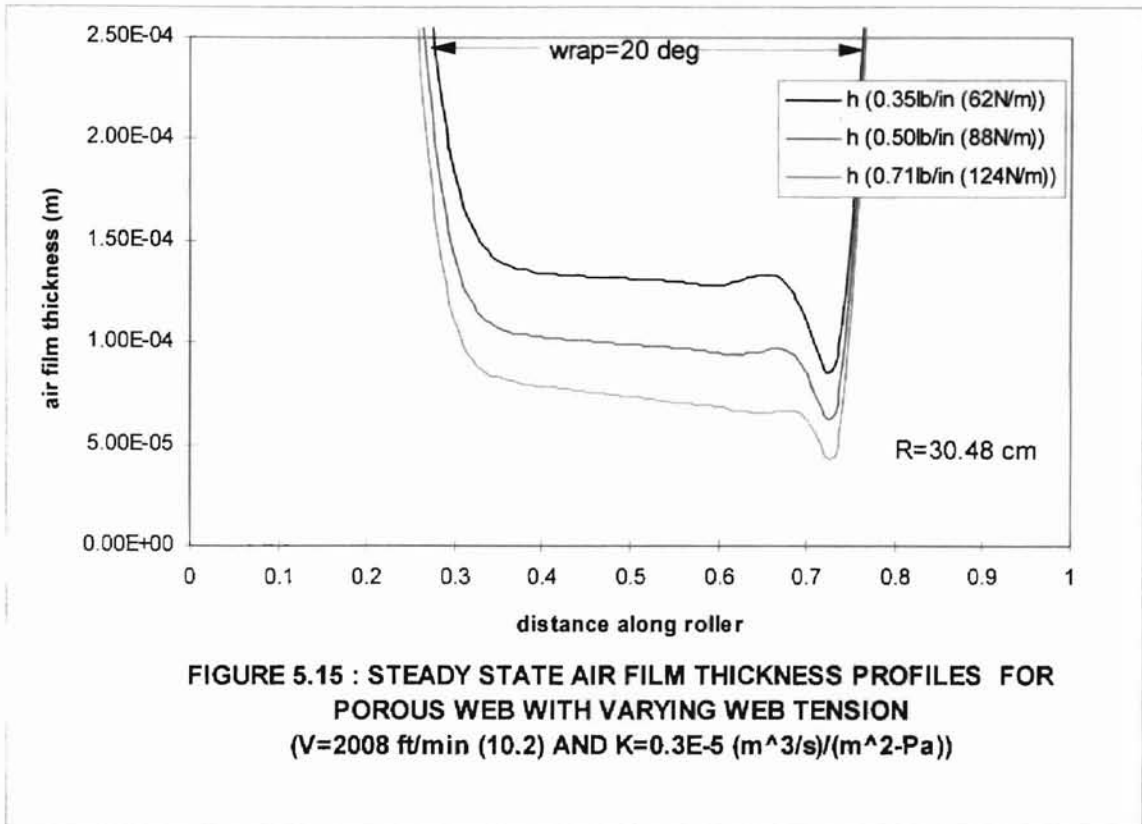
$$h = 0.643R \left[\frac{6\mu(V_R + V_W)}{T} \right]^{2/3} - 2 \left[\frac{KT}{(V_R + V_W)} \right] \theta \quad (5.1)$$

where, θ is the spatial coordinate in radians and K is the web permeability. This equation is based on the assumptions that the pressure in the decreasing gap remains constant and the velocity of the air flowing through the web is also constant. As observed from this present study, these assumptions hold good for typical operating parameters and web permeabilities .

The driving force on the entrapped air through the porous web is the difference $(p-p_a)$ between the air film pressure, p and the ambient pressure, p_a . The difference in pressure $(p-p_a)$ in the air film is directly proportional to web tension, T . Figure 5.15 displays air gap profiles for varying web tension. The slope (m/radian) of the decreasing central region air gap profile decreases with the decrease in web tension. With the decrease in web tension the driving force on the entrapped air decreases and the amount of entrained air flowing through the porous web also decreases. This can be explained considering the ratio of air flowing across the web to the amount of air entrapped between the roller and the web surfaces. As we have seen earlier, the lower the tension, the more air is entrained between the web and the roller surfaces than for the case of higher web tension. Thus for situations when the ratio of air flowing across the web to the amount of air entrapped between the roller and the web surfaces is low the slope of the decreasing air gap profile is small and vice versa. Figure 5.16 displays air gap profiles for varying web velocities. For higher web velocity more air is entrained between the roller and the web surfaces and therefore the ratio of air flowing through the web to the amount of air entrapped is low as compared to the case of lower web velocity. Thus, the greater slope of the decreasing central region air gap profile is expected for lower web velocities as compared to higher web velocities at the same web tension and web permeability.

Comparisons of the central region air-film profiles are made with the air film heights given by equation (5.1) and are displayed in Figures 5.17, 5.18 and 5.19. The two results are in good agreement and the maximum percentage difference calculated for the three different cases presented is 1.21%. The slopes of the decreasing air gap profiles are

also in very close agreement for the two analyses compared. The dip of the web at the exit region is also analyzed for the case of a porous web compared to the case of a non-porous web. Results displayed in Figures 5.20 and 5.21 show that for porous webs the minimum air gap at the exit region is less than non-porous webs because of the entrained air flowing out through the porous webs. However in none of the cases studied here was the web observed touching the roller at the exit region, which can occur for very porous webs as documented by Ducotey and Good [1996]. Also note that the permeability used in this study were chosen only to make a theoretical comparison. The air film thicknesses in the entrance region are quite large ($0.75e-04$ to $1.25e-04$ m) and side leakage may contribute as much to air film loss as permeability depending upon web width as noted by Ducotey and Good [1996].



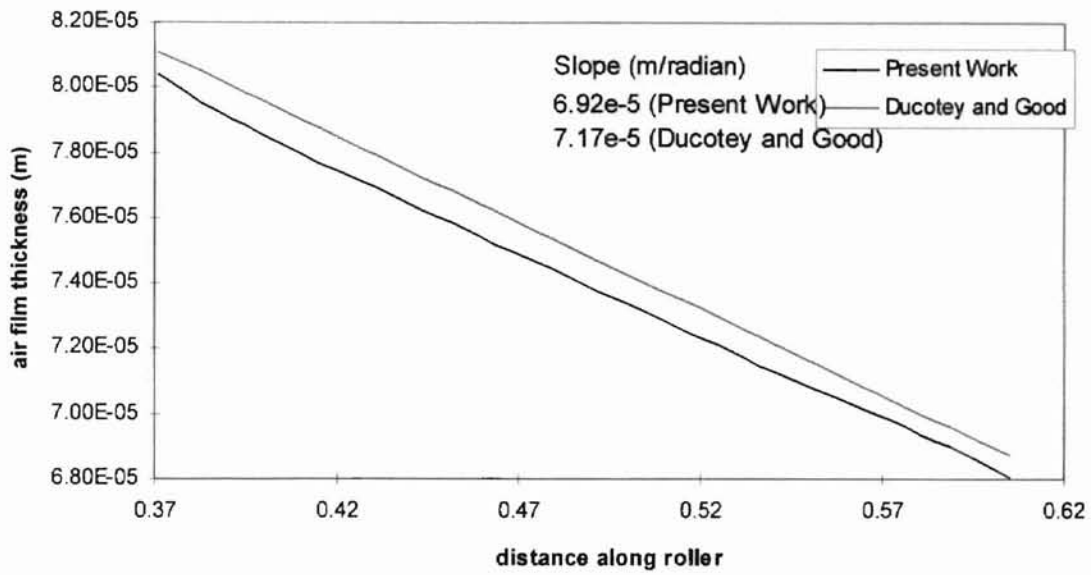


FIGURE 5.17 : COMPARISON OF THE AIR FILM THICKNESS PROFILE FOR POROUS WEB (CENTRAL REGION)
 (V=2008 ft/min (10.2), T=0.71 lb/in (124) AND K=0.3E-5 (m³/s)/(m²-Pa))

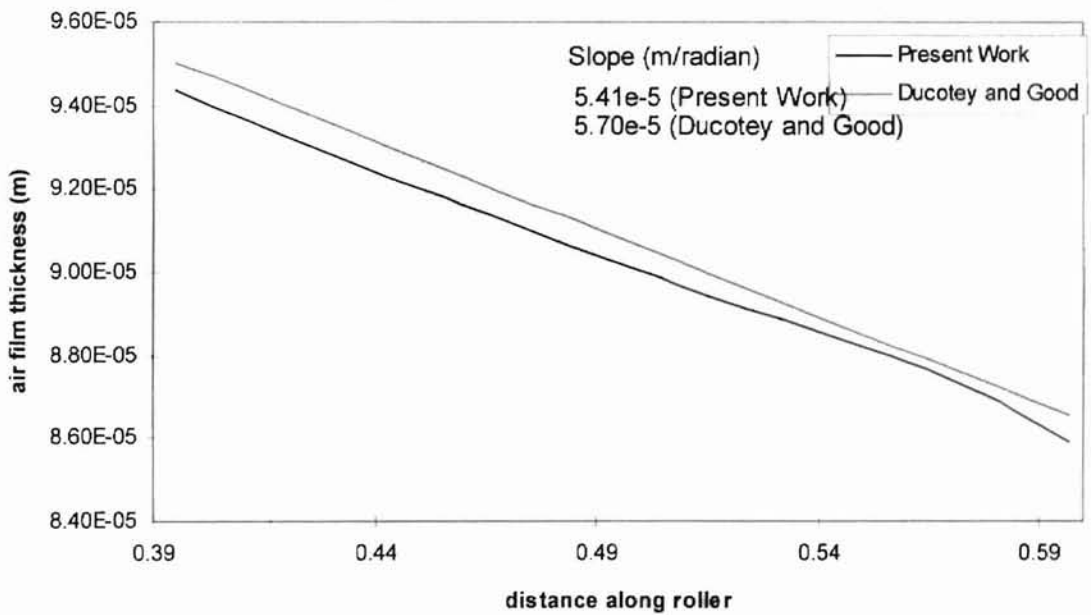


FIGURE 5.18 : COMPARISON OF THE AIR FILM THICKNESS PROFILE FOR POROUS WEB (CENTRAL REGION)
 (V=2500 ft/min (12.7), T=0.71 lb/in (124) AND K=0.3E-5 (m³/s)/(m²-Pa))

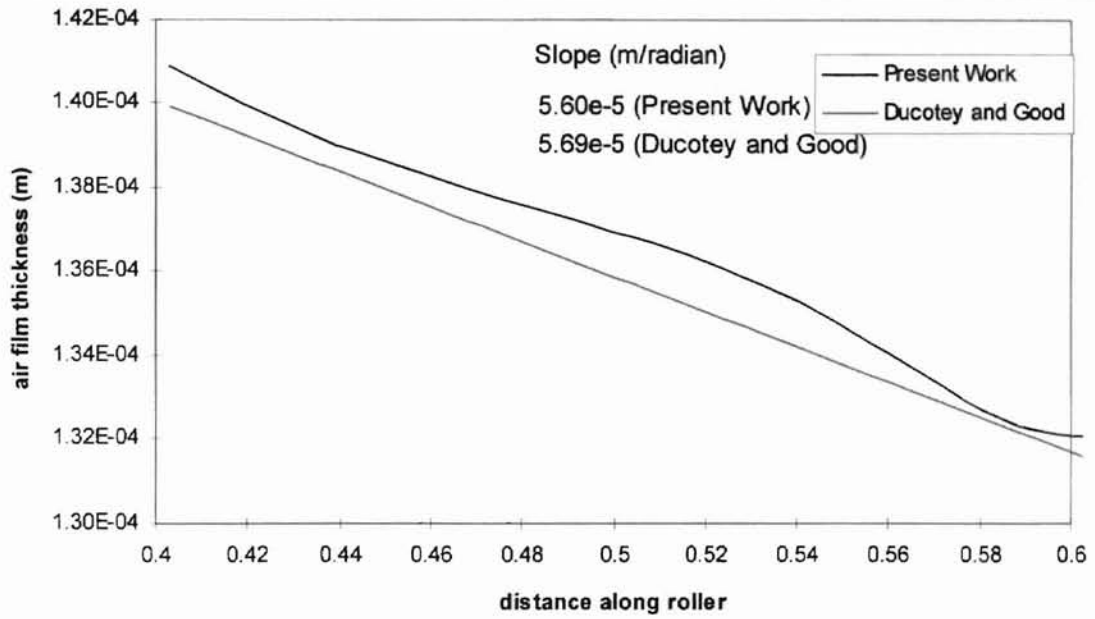


FIGURE 5.19 : COMPARISON OF THE AIR FILM THICKNESS PROFILE FOR POROUS WEB (CENTRAL REGION)
 (V=2992 ft/min (15.2), T=0.5 lb/in (88) AND K=0.52E-5 (m³/s)/(m²-Pa))

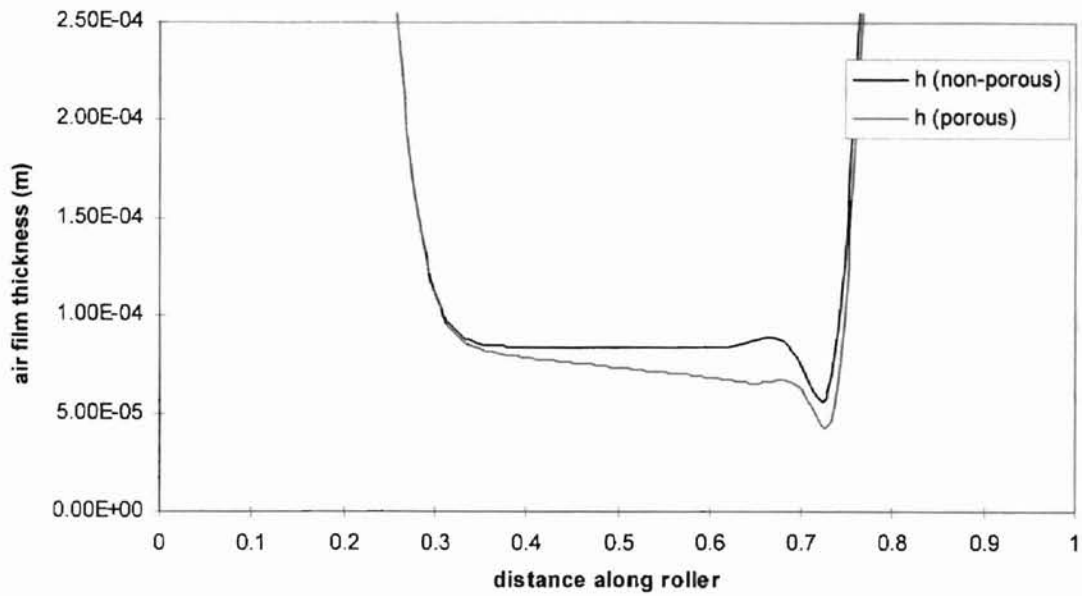


FIGURE 5.20 : COMPARISON OF EXIT REGION AIR FILM THICKNESS PROFILE FOR NONPOROUS AND POROUS ($K=0.3E-5 \text{ (m}^3\text{/s)/(\text{m}^2\text{-Pa)}$) WEB ($V=2008 \text{ ft/min (10.2)}$ AND $T=0.71 \text{ lb/in (124)}$)

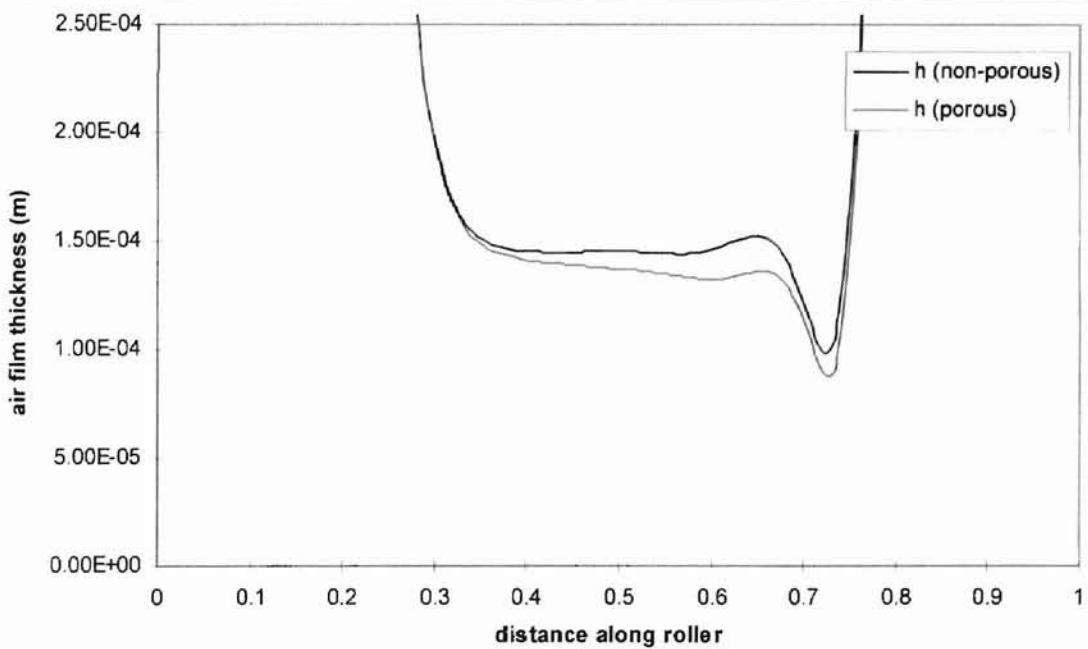


FIGURE 5.21 : COMPARISON OF EXIT REGION AIR FILM THICKNESS PROFILE FOR NONPOROUS AND POROUS ($K=0.52E-5 \text{ (m}^3\text{/s)/(\text{m}^2\text{-Pa)}$) WEB ($V=2992 \text{ ft/min (15.2)}$ AND $T=0.50 \text{ lb/in (88)}$)

5.3 Summary

It is seen from the earlier discussion that efficient web processing and web quality critically depend upon having a proper air film thickness between a moving web and a drive or support roller. An inadequate air film results in web damage due to abrasion and an excessive air film results in loss of drive traction and lateral positioning control. Computational results presented in the previous two sections (5.1 and 5.2) show the effects of various web properties and web-roller parameters on the lubricating air film thickness between a moving web and a smooth roller. Results for non-porous webs show that more air is entrained between the web and roller surface as the web velocity increases indicating a possible reduction in web-roller traction. The same is the case for increasing roller diameter. On the other hand increasing web tension may increase the traction by reducing the air film thickness and increasing the asperity contact, and increasing the length of the constant gap central region. The density of the web can play a significant role at high web velocities as a denser web entrains more air adding to the effect of increasing web velocity. The effect of the rotating roller is to effectively increase the net velocity thus entraining more air. It is also seen that the effect of slip flow is to reduce the air film thickness. The results display the characteristic exponential decrease in air film thickness for the entrance region, constant thickness in the central region, and sinusoidal behavior at the exit region. The results for porous webs display nearly linear reduction in central region air film thickness with distance along the roller. The slope of the decreasing air film gap depends upon web tension, web-roller velocity and web permeability and the analysis shows that the slope will increase with angular position.

However, for typical operating parameters and web permeabilities this change in slope is small. Also, for porous webs the minimum air gap at the exit region is less than non-porous webs because of the entrained air flowing out through the porous webs.

CHAPTER VI

CONCLUSIONS AND RECOMMENDATIONS

6.1 Conclusions

The following conclusions can be drawn from the present study:

1. The transient response of the air film thickness indicates that the transient period depends upon the web-roller velocity, wrap angle and roller radius.
2. The effect of slip flow is to reduce the air film gap when compared with the no slip case. However, for most web handling applications the mean free path of air is very small compared to the air film thickness, hence slip flow effects usually can be neglected.
3. Increasing web tension reduces the air-film gap and increases the length of the constant gap central region.
4. More air is entrained between the web and roller surfaces with increasing web-roller velocity implying a possible reduction in the web-roller traction.
5. For similar operating conditions more air is entrained as the density of web increases adding to the effect of increasing web-roller velocity.
6. A rotating roller adds to the net velocity thus entraining more air than the stationary roller case.
7. For the case of porous webs the central region air film thickness profile displays a nearly linear decrease along the roller or the wrap angle. The slope of the decreasing

- air film gap depends upon web tension, web-roller velocity and web permeability and increases slightly with angular position.
8. The minimum air gap at the exit region is less for porous webs compared to non-porous webs for similar operating conditions.
 9. More air is entrained with increasing roller radius.
 10. Steady state air film thickness profiles display an exponentially decreasing entrance region, constant gap central region (for nonporous webs), and sinusoidal varying exit region, where the constant gap region thickness matches the foil bearing prediction.

6.2 Recommendations for Future Work

Based on the present study the following suggestions are worth considering for the future work :

1. In order to establish the validation of the present numerical model, it is recommended that experiments be performed with nonporous and porous webs on supporting rollers of different radii. Measurements must be taken at all the three regions of web-roller interface, 1. inlet region, 2. central region, and 3. exit region.
2. The limitation of this model is that it does not take into account the effects of the flexibility of the web material. The inclusion of this affect will enable us to determine the effects of web stiffness on air film thickness.
3. As it has been observed by past researchers that grooved rollers are effective in reducing the air film thickness. It is recommended for future work to incorporate a grooved roller model to numerically study the effects of grooved rollers on the entrapped air film.

4. More review is needed to incorporate the effect of side leakage in the case of a finite width web-roller interface.
5. It is recommended to study the effects of squeeze film analysis in the roll winding process.

SELECTED BIBLIOGRAPHY

1. Adams, G.G., "A Novel Approach to the Foil Bearing Problem," Tribology and Mechanics of Magnetic Storage Systems, ASLE Special Publication 22, pp. 1-7, 1987.
2. Barlow, E.J., "Derivation of Governing Equations for Self-Acting Foil Bearings," Trans. of ASME, Journal of Lubrication Technology, Vol. 89, pp. 334-340, 1967.
3. Basheer, M.S., "An Experimental study of Air Entrainment in Web Handling Applications," M.S. Thesis, School of Mechanical and Aerospace Engineering, Oklahoma State University, 1988.
4. Benson, R.C., "The Slippery Sheet," Trans. of ASME, Journal of Tribology, Vol. 117, pp. 47-52, 1995.
5. Bhushan, B., and Tonder, K., "Roughness-Induced Shear and Squeeze-Film Effects in Magnetic Recording - Part I&II," Trans. of ASME, Journal of Tribology, Vol. 111, pp. 220-237, 1989.
6. Bhushan, B., Tribology and Mechanics of Magnetic Storage Devices, Springer-Verlag, New York, Chapter 9, 1990.
7. Brewen, A.T., Benson, R.C., and Piarulli, V.J., "A Simple Procedure for Determining Elastohydrodynamic Equilibrium and Stability of a Flexible Tape Flying Over a Recording Head," Tribology and Magnetic Storage Systems, Vol. II, ASLE Special Publication SP-19, editors, B. Bhushan and N.S. Eiss Jr., pp. 43-51, 1985.
8. Brundertt, E., and Baines, W.D., "The Flow of Air Through Wet Paper," TAPPI Journal, Vol. 49, No. 3, pp. 97-101, March, 1966.
9. Dais, J.L., and Barnum, T.B., "The Geometrically Irregular Foil Bearing," ASME Journal of Lubrication Technology, Vol. 96, pp. 224-227, 1974.
10. Daly, D.A., "Factors Controlling Traction Between Webs and Their Carrying Rolls," TAPPI Journal, pp. 88A-90A, Vol. 48, September, 1965.
11. Ducotey, K.S., and Good, J.K., "The Effect of Web Permeability and Side Leakage on the Air Film Height Between a Roller and Web," Submitted for Review for Publication in The Journal of Tribology, January, 1996.

12. Eshel, A., "Analytical Study of the Self-Acting Foil Bearing," Ph.D. Dissertation, Department of Mechanical Engineering, Columbia University, New York, May, 1966.
13. Eshel, A., "Compressibility Effects on the Infinitely Wide, Perfectly Flexible Foil Bearing," ASME Journal of Lubrication Technology, Vol. 90, pp. 221-225, 1968.
14. Eshel, A., "The Propagation of Disturbances in the Infinitely Wide Foil Bearing," ASME Journal of Lubrication Technology, Vol. 91, pp. 120-125, 1969.
15. Eshel, A., "On Controlling the Film Thickness in Self-Acting Foil Bearings," ASME Journal of Lubrication Technology, Vol. 92, pp. 359-362, 1970.
16. Eshel, A., "On Fluid Inertia Effects in Infinitely Wide Foil Bearings," ASME Journal of Lubrication Technology, Vol. 92, pp. 490-494, 1970.
17. Eshel, A., "Reduction of Air Films in Magnetic Recording by External Air Pressure," ASME Journal of Lubrication Technology, Vol. 96, pp. 247-249, 1974.
18. Eshel, A., and Elrod, H.G., Jr., "The Theory of the Infinitely Wide, Perfectly Flexible, Self-Acting Foil Bearing," ASME Journal of Basic Engineering, Vol. 87, No. 4, pp. 831-836, 1965.
19. Eshel, A., and Lowe, A.R., "Experimental and Theoretical Investigation of Head to Tape Separation in Magnetic Recording," IEEE Trans. on Magnetics, Vol. MAG-9, No. 4, pp. 683-688, 1973.
20. Eshel, A., and Wildmann, M., "Dynamic Behavior of a Foil in the Presence of a Lubricating Film," ASME Journal of Applied Mechanics, Vol. 35, pp. 242-247, 1968.
21. Forsythe, G.E., and Wasow, W.R., Finite Difference Methods for Partial Differential Equations, John Wiley & Sons, Inc., New York, pp. 103-105, 1960.
22. Granzow, G.D., "An Improved Foil Bearing Solution," M.S.Thesis, Department of Mechanical Engineering, University of New Mexico, 1980.
23. Granzow, G.D., and Lebeck, A.O., "An Improved One-Dimensional Foil Bearing Solution," Tribology and Mechanics of Magnetic Storage Systems, ASLE Special Publication 16, pp. 54-58, 1984.
24. Gross, W.A., Matsch, L.A., Castelli, V., Eshel, A., Vohr, J.H., and Wildmann, M., Fluid Film Lubrication, John Wiley & Sons, Inc., NY, 1980.
25. Hamza, E.A., and MacDonald, D.A., "A Fluid Film Squeezed Between Two Parallel Plane Surfaces," Journal of Fluid Mech., Vol. 109, pp. 147-160, 1981.

26. Hashemi, S.M., and Roylance, B.J., "Analysis of an Oscillatory Oil Squeeze Film Including Effects of Fluid Inertia," Tribology Trans., Vol. 32, pp. 461-468, 1989.
27. Hashimoto, H., "Viscoelastic Squeeze Film Characteristics with Inertia Effects Between Two Parallel Circular Plates Under Sinusoidal Motion," Trans. of ASME, Journal of Tribology, Vol. 116, pp. 161-166, 1994.
28. Hays, D.F., "Squeeze Film for Rectangular Plates," Trans. of ASME, Journal of Basic Engineering, Vol. 85, pp. 243-246, 1963.
29. Heinrich, J.C., and Connolly, D., "Three-Dimensional Finite Element Analysis of Self-Acting Foil Bearing," Computer Methods in Applied Mechanics and Engineering, Vol. 100, pp. 31-43, 1992.
30. Heinrich, J.C., and Wadhwa, S.K., "Analysis of Self-Acting Foil Bearings: A Finite Element Approach," Tribology and Mechanics of Magnetic Storage Systems, Vol. III, editors, B. Bhushan, and N.J. Eiss Jr., pp. 152-159, 1986.
31. Jones, A.F., and Wilson, S.D., "On the Failure of Lubrication Theory in Squeezing Flows," Trans. of ASME, Journal of Lubrication. Tech., Vol. 97, pp. 101-104, 1975.
32. Knox, K.L., and Sweeney, T.L., "Fluid Effects Associated With Web Handling," Ind. Eng. Chem. Process. Design. Dev., Vol. 10, pp. 201-205, 1971.
33. Lilley, D.G., Computational Fluid Dynamics, Vol. 1, Chapter 9, 1992.
34. Randall, W., and Weinbaum, S., "On the Development of Fluid Trapping Beneath Deformable Fluid-Cell Membranes," Journal of Fluid Mech., Vol. 121, pp. 315-343, 1982.
35. Riddiford, A.W., "Airflow Between a Paper and a Dryer Surface," TAPPI Journal, Vol. 52, No. 5, pp. 939-942, 1969.
36. Riddiford, A.W., "Air Entrainment Between an Impermeable Paper Web and Dryer Surface of Infinite Width," Pulp and Paper Magazine of Canada, pp. 53-57, February 7, 1969.
37. Rohde, S., Whicker, D., and Browne, A.L., "Dynamic Analysis of Elastohydrodynamic Squeeze Films," Trans. of ASME, Journal Of Lubrication. Tech., Vol. 98, pp. 401-407, 1976.
38. Rongen, P.M.J., "On Numerical Solution of the Instationary 2D Foil Bearing Problem," Tribology and Mechanics of Magnetic Storage Systems, ASLE Special Publication 26, pp. 130-138, 1989.

39. Smith, D.P., and Von Behren, R.A., "Squeeze-Film Analysis of Tape Winding Effects in Data Cartridge," Tribology and Magnetic Storage Systems, Vol. VI, STLE Special Publication SP-26, editors, B. Bhushan and N.S. Eiss Jr., pp. 88-92, 1989.
40. Stahl, K.J., White, J.W., and Deckert, K.L., "Dynamic Response of Self-Acting Foil Bearings," IBM J. Res. Development, Vol. 18, pp. 513-520, 1974.
41. Tanaka, K., "Analytical and Experimental Study of Tape Spacing for Magnetic Tape Unit - Effects of Tape Bending Rigidity, Gas Compressibility, and Molecular Mean Free Path," Tribology and Mechanics of Magnetic Storage Systems, ASLE Special Publication 19, pp. 72-79, 1985.
42. Tanaka, K., Oura, M., and Fujii, M., "Tape Spacing Characteristics of Cylindrical Heads With Taped Flat Surfaces for Use in Magnetic Tape Units," Tribology and Mechanics of Magnetic Storage Systems, Vol. III, editors, B. Bhushan, and N.J. Eiss Jr., pp. 130-137, 1986.
43. Tichy, J.A., and Winer, W.O., "Inertial Considerations in Parallel Circular Squeeze Film Bearings," Trans. of ASME, Journal of Lubrication. Tech., Vol. 92, pp. 588-592, 1970.
44. Von Behren, R.A., and Smith, D.P., "Squeeze-Film Analysis of Tape Winding Effects in Data Cartridge," Tribology and Mechanics of Magnetic Storage Systems, ASLE Special Publication 26, pp. 88-92, 1989.
45. Watanabe, Y., and Sueoka, Y., "Evaluation of Air Entrainment Between a Paper Web and a Roller," Presented at Technical Association of the Graphic Arts, Kansas City, Mo., 1990.
46. Weinbaum, S., Lawrence, C.J., and Kuang, Y., "The Inertial Draining of a Fluid Layer Between Parallel Plates with a Constant Normal Force - Part I," Journal of Fluid Mech., Vol. 156, pp. 463-477, 1985.
47. Weinbaum, S., Lawrence, C.J., and Kuang, Y., "The Inertial Draining of a Fluid Layer Between Parallel Plates with a Constant Normal Force - Part II," Journal of Fluid Mech., Vol. 156, pp. 479-494, 1985.
48. Wickert, J.A., "Free Linear Vibration of Self-Pressurized Foil Bearings," ASME Journal of Vibration and Acoustics, Vol. 115, pp. 145-151, 1993.
49. Yamauchi, T., Murakami, K., and Imamura, R., "The Air Permeability of Paper Related to the Porous Structure," Japan TAPPI Journal, Vol. 30, No. 5, pp. 273-280, 1976.

50. Yang, S., and Leal, L.G., "Thin Fluid Film Squeezed with Inertia Between Two Parallel Plane Surfaces," Trans. of ASME, Journal of Tribology, Vol. 115, pp. 632-639, 1993.

APPENDIX A

Reynolds Lubrication equation for nonporous web with stationary roller
(considering slip flow)

The velocity profile of the air entrained between the web and the roller surface is-

$$V = \frac{1}{2\mu} \frac{\partial p}{\partial x} y^2 + C_1 y + C_2 \quad (1)$$

Thus,

$$\frac{\partial V}{\partial y} = \frac{1}{\mu} \frac{\partial p}{\partial x} y + C_1 \quad (2)$$

Using the boundary conditions-

$$V|_{y=0} = \lambda \left. \frac{\partial V}{\partial y} \right|_{y=0}$$

and,

$$V|_{y=h} = V - \lambda \left. \frac{\partial V}{\partial y} \right|_{y=h} \quad (3)$$

Using the first boundary condition in equation (1) and(2) yields-

$$C_2 = \lambda C_1$$

The second boundary condition yields,

$$\frac{1}{2\mu} \frac{\partial p}{\partial x} h^2 + C_1 h + C_2 = V - \lambda \left(\frac{1}{\mu} \frac{\partial p}{\partial x} h + C_1 \right)$$

$$\Rightarrow \frac{1}{2\mu} \frac{\partial p}{\partial x} h^2 + C_1 h + \lambda C_1 = V - \lambda C_1 - \frac{\lambda}{\mu} \frac{\partial p}{\partial x} h$$

$$\Rightarrow C_1(2\lambda + h) = V - \frac{\lambda}{\mu} \frac{\partial p}{\partial x} h - \frac{1}{2\mu} \frac{\partial p}{\partial x} h^2$$

$$\Rightarrow C_1 = \frac{V - \frac{h}{2\mu}(h + 2\lambda) \frac{\partial \phi}{\partial x}}{(h + 2\lambda)}$$

Thus,

$$C_2 = \lambda C_1$$

Now,

$$Q = \rho \int_{y=0}^{y=h} \left(\frac{1}{2\mu} \frac{\partial \phi}{\partial x} y^2 + C_1 y + C_2 \right) dy$$

$$\Rightarrow Q = \rho \left(\frac{1}{6\mu} \frac{\partial \phi}{\partial x} h^3 + C_1 \frac{h^2}{2} + C_2 h \right)$$

Substituting $C_2 = \lambda C_1$ yields,

$$Q = \rho \left(\frac{1}{6\mu} \frac{\partial \phi}{\partial x} h^3 + \frac{C_1 h}{2} (h + 2\lambda) \right)$$

Substituting for C_1 yields,

$$= \rho \left(\frac{1}{6\mu} \frac{\partial \phi}{\partial x} h^3 + \frac{h}{2} \left(V - \frac{h}{2\mu} (h + 2\lambda) \frac{\partial \phi}{\partial x} \right) \right)$$

On simplification this yields,

$$Q = \rho \left[\frac{Vh}{2} - \frac{1}{12\mu} \frac{\partial \phi}{\partial x} h^3 - \frac{1}{2\mu} \frac{\partial \phi}{\partial x} h^2 \lambda \right] \text{ which is equation (3.11) in the text.}$$

APPENDIX B

Reynolds Lubrication equation for porous web with rotating roller

(considering no slip flow)

The velocity equation is given by-

$$V = \frac{1}{2\mu} \frac{\partial \phi}{\partial x} y^2 + C_1 y + C_2 \quad (1)$$

for the case of rotating roller and moving web the following boundary conditions applies,

for no slip condition considering V_R to be the roller surface velocity and V_w to be the web velocity,

$$V|_{y=0} = V_R$$

and,

$$V|_{y=h} = V_w$$

Substituting the above two conditions in equation(1) yields,

$$V_R = C_2$$

and,

$$V_w = \frac{1}{2\mu} \frac{\partial \phi}{\partial x} h^2 + C_1 h + C_2$$

$$\Rightarrow V_w = \frac{1}{2\mu} \frac{\partial \phi}{\partial x} h^2 + C_1 h + V_R$$

Solving which yields,

$$C_1 = \frac{\left(V_w - V_R - \frac{1}{2\mu} \frac{\partial \phi}{\partial x} h^2 \right)}{h} \text{ and,}$$

$$C_2 = V_R$$

Now,

$$Q = \rho \int_{y=0}^{y=h} \left(\frac{1}{2\mu} \frac{\partial p}{\partial x} y^2 + C_1 y + C_2 \right) dy$$

$$\Rightarrow Q = \rho \left(\frac{1}{6\mu} \frac{\partial p}{\partial x} h^3 + C_1 \frac{h^2}{2} + C_2 h \right)$$

Substituting for C_1 and C_2 yields,

$$Q = \rho \left[\frac{1}{6\mu} \frac{\partial p}{\partial x} h^3 + \left(\frac{V_w - V_r - \frac{1}{2\mu} \frac{\partial p}{\partial x} h^2}{h} \right) \frac{h^2}{2} + V_r h \right]$$

Upon simplification this yields,

$$Q = \rho \left[\frac{h}{2} (V_r + V_w) - \frac{1}{12\mu} \frac{\partial p}{\partial x} h^3 \right]$$

Now for case of a porous web referring to Figure 3.5 we can say

$$Q_{in} - Q_{out} = Q_{thru} + \frac{\partial}{\partial t} (\rho h \Delta x)$$

$$Q_{in} - Q_{out} = \rho V_i (\Delta x) + \frac{\partial}{\partial t} (\rho h \Delta x)$$

where,

V_i = velocity of air through the porous web, and

ρ = air density.

This can be further simplified as,

$$-\frac{\partial Q}{\partial x} = \frac{\partial}{\partial t} (\rho h) + \rho V_i$$

Substituting for Q and using the ideal gas relation at constant temperature, $\rho \propto p$ yields,

$$-\frac{\partial}{\partial x} \left[p \left(\frac{h}{2} (V_R + V_w) - \frac{1}{12\mu} \frac{\partial p}{\partial x} h^3 \right) \right] = \frac{\partial}{\partial t} (ph) + pV_i$$

This can be further simplified as the following differential equation-

$$(h^3 pp_x)_x = 6\mu(V_R + V_w)(ph)_x + 12\mu(ph)_t + 12\mu pV_i$$

Considering the slip flow case, the term $6\lambda_a p_a (h^2 p_x)_x$ as in case derived for nonporous web in Appendix A will be included further refining the equation to-

$$(h^3 pp_x)_x + 6\lambda_a p_a (h^2 p_x)_x = 6\mu(V_R + V_w)(ph)_x + 12\mu(ph)_t + 12\mu pV_i$$

APPENDIX C

Finite difference formulation of the two governing equations

(Foil motion equation and Reynolds Lubrication equation)

Finite difference operators used --

$$y_{xx} = (y_{i+1}^{n+1} - 2y_i^{n+1} + y_{i-1}^{n+1})/\Delta x^2$$

$$y_{tt} = (y_i^{n+1} - 2y_i^n + y_i^{n-1})/\Delta t^2$$

$$y_{xt} = (y_{i+1}^{n+1} - y_{i+1}^{n-1} - y_{i-1}^{n+1} + y_{i-1}^{n-1})/4\Delta x\Delta t$$

$$p_x = (p_{i+1}^{n+1} - p_{i-1}^{n+1})/2\Delta x$$

$$p_t = (p_i^{n+1} - p_i^n)/\Delta t$$

$$p_{xx} = (p_{i-1}^{n+1} - 2p_i^{n+1} + p_{i+1}^{n+1})/\Delta x^2$$

$$h_x = (h_{i+1}^{n+1} - h_{i-1}^{n+1})/2\Delta x$$

$$h_t = (h_i^{n+1} - h_i^n)/\Delta t$$

1. Foil motion equation --

$$\rho b \left(\frac{\partial^2 y}{\partial t^2} + 2V_w \frac{\partial^2 y}{\partial x \partial t} + V_w^2 \frac{\partial^2 y}{\partial x^2} \right) - \frac{T}{w} \frac{\partial^2 y}{\partial x^2} = p - p_a$$

This can also be written in the following form-

$$\rho b (y_{tt} + 2V_w y_{xt} + V_w^2 y_{xx}) - \frac{T}{w} y_{xx} = p - p_a$$

After substituting proper finite difference operators for the derivatives and solving, this yields an implicit formulation of the type-

$$B_1 y_{i-1}^{n+1} + D_1 y_i^{n+1} + A_1 y_{i+1}^{n+1} = E_1$$

where,

$$B_1 = \left[\frac{-\rho b V_w}{2\Delta x \Delta t} + \frac{\rho b V_w^2}{\Delta x^2} - \frac{T/w}{\Delta x^2} \right]$$

$$D_1 = \left[\frac{\rho b}{\Delta t^2} - \frac{2\rho b V_w^2}{\Delta x^2} + \frac{2T/w}{\Delta x^2} \right]$$

$$A_1 = \left[\frac{\rho b V_w}{2\Delta x \Delta t} + \frac{\rho b V_w^2}{\Delta x^2} - \frac{T/w}{\Delta x^2} \right]$$

and,

$$E_1 = \left\{ (p_i^n - p_a) + \left[\left(\frac{2\rho b}{\Delta t^2} \right) y_i^n - \left(\frac{\rho b}{\Delta t^2} \right) y_i^{n-1} + \left(\frac{\rho b V_w}{2\Delta x \Delta t} \right) y_{i+1}^{n-1} - \left(\frac{\rho b V_w}{2\Delta x \Delta t} \right) y_{i-1}^{n-1} \right] \right\}$$

2. Reynolds Lubrication equation --

$$\frac{\partial}{\partial x} \left(h^3 p \frac{\partial p}{\partial x} \right) + 6\lambda_a p_a \frac{\partial}{\partial x} \left(h^2 \frac{\partial p}{\partial x} \right) = 6\mu(V_r + V_w) \frac{\partial}{\partial x} (ph) + 12\mu \frac{\partial}{\partial t} (ph) + 12\mu Kp(p - p_a)$$

This can be also expressed as-

$$\begin{aligned} & \left(h^3 p p_{xx} + h^3 p_x^2 + 3h^2 p p_x h_x \right) + 6\lambda_a p_a \left(h^2 p_{xx} + 2h p_x h_x \right) = \left[12\mu (p h_t + h p_t) \right. \\ & \left. + 6(V_r + V_w) \mu (p_x h + h_x p) + 12\mu Kp(p - p_a) \right] \end{aligned}$$

After substituting proper finite difference operators for the derivatives and solving, this yields an implicit formulation of the type-

$$B_2 p_{i-1}^{n+1} + D_2 p_i^{n+1} + A_2 p_{i+1}^{n+1} = E_2$$

where,

$$B_2 = \left\{ \begin{aligned} & \left(\frac{-6\mu(V_R + V_W)h_i^{n+1}}{2\Delta x} \right) - \left(\frac{(h_i^{n+1})^3 p_i^n}{\Delta x^2} \right) + \left(\frac{(h_i^{n+1})^3 (p_{i+1}^n - p_{i-1}^n)}{4\Delta x^2} \right) \\ & + \left(\frac{3(h_i^{n+1})^2 p_i^n (h_{i+1}^{n+1} - h_{i-1}^{n+1})}{4\Delta x^2} \right) - \left(\frac{6\lambda_a p_a (h_i^{n+1})^2}{\Delta x^2} \right) + \left(\frac{6\lambda_a p_a h_i^{n+1} (h_{i+1}^{n+1} - h_{i-1}^{n+1})}{2\Delta x^2} \right) \end{aligned} \right\}$$

$$D_2 = \left\{ \begin{aligned} & \left(\frac{12\mu(2h_i^{n+1} - h_i^n)}{\Delta t} \right) + \left(\frac{3\mu(V_R + V_W)(h_{i+1}^{n+1} - h_{i-1}^{n+1})}{\Delta x} \right) + \left(\frac{2(h_i^{n+1})^3 p_i^n}{\Delta x^2} \right) \\ & + 6\lambda_a p_a \left(\frac{2(h_i^{n+1})^2}{\Delta x^2} \right) + 12\mu K(p_i^n - p_a) \end{aligned} \right\}$$

$$A_2 = \left\{ \begin{aligned} & \left(\frac{6\mu(V_R + V_W)h_i^{n+1}}{2\Delta x} \right) - \left(\frac{(h_i^{n+1})^3 p_i^n}{\Delta x^2} \right) - \left(\frac{(h_i^{n+1})^3 (p_{i+1}^n - p_{i-1}^n)}{4\Delta x^2} \right) - \\ & \left(\frac{3(h_i^{n+1})^2 p_i^n (h_{i+1}^{n+1} - h_{i-1}^{n+1})}{4\Delta x^2} \right) - 6\lambda_a p_a \left(\frac{h_i^{n+1} (h_{i+1}^{n+1} - h_{i-1}^{n+1})}{2\Delta x^2} + \frac{(h_i^{n+1})^2}{\Delta x^2} \right) \end{aligned} \right\}$$

and,

$$E_2 = \left\{ \left(\frac{12\mu p_i^n h_i^{n+1}}{\Delta t} \right) \right\}$$

APPENDIX D

Computer code for the computations of the air film thickness and pressure distribution

```

C*****
C  MAE- THESIS
C  OKLAHOMA STATE UNIVERSITY

C  NUMERICAL MODEL TO PREDICT THE AIR-GAP AND THE PRESSURE
C  DISTRIBUTION BETWEEN MOVING WEBS AND SUPPORT ROLLERS

C  BY- KOTHARI, SATYANARAYAN

C*****
C  DEFINING THE VARIABLE USED IN THIS PROGRAM.

C  X - DISTANCE ALONG THE ROLLER(i.e. LONGITUDINAL DIRECTION).
C  Y - DISPLACEMENT OF THE FOIL OR WEB FROM THE EQUILIBRM
C  POSITION W.R.T. X(i.e. ALONG LONGITUDINAL DIRECTION)
C  AND TIME T.
C  P - PRESSURE DISTRIBUTION BETWEEN THE FOIL AND THE ROLLER
C  W.R.T. X(i.e. ALONG LONGITUDINAL DIRECTION) AND TIME T.
C  PA - AMBIENT PRESSURE
C  PR - (P-PA)
C  H - AIR FILM GAP BETWEEN THE ROLLER AND THE FOIL.
C  HO - INITIAL AIR FILM THICKNESS.
C  PO - INITIAL PRESSURE DISTRIBUTION.
C  M - MASS PER UNIT WIDTH PER UNIT LENGTH OF THE FOIL(Kg/m^2).
C  T - TENSION PER UNIT WIDTH APPLIED ON THE FOIL(N/m).
C  V - VELOCITY WITH WHICH THE FOIL IS MOVING(m/s).
C  AK - PERMEABILITY((m^3/s)/(m^2-Pa)).
C  R - ROLLER RADIUS(m).
C  VR - ROLLER SURFACE VELOCITY(m/s).
C  LE - LENGTH BETWEEN TWO END SUPPORTING ROLLERS(m).
C  MU - VISCOSITY OF AIR(N/(m^2-s)).
C  LAM - MEAN FREE PATH OF AIR(m).
C  DEL - DESCRIBES THE ROLLER PROFILE.
C  DELX - MESH SIZE IN THE X DIRECTION.
C  DELT - TIME STEP (s)
C  A,AA,B,BB,C,CC,D,DD - ARE THE VARIABLE USED FOR STORING THE
C  ELEMENTS OF THE TRI-DIAGONAL MATRICES
C  FOR THE TWO GOVERNING EQUATIONS.
C*****
PROGRAM FOIL
IMPLICIT DOUBLE PRECISION (A-Z)
INTEGER I,J,ITER,ITERM,NN,N,II,ITERP,DELPR,N1,N2,ISYSTEM
DIMENSION DEL(125),X(125),Y(125,5),H(125,5),P(125),PR(125)
DIMENSION A(125),B(125),C(125),D(125)
DIMENSION AA(125),BB(125),CC(125),DD(125)
CHARACTER FLNAME *15
DATA MU,PA,DELT/1.81E-5,8.41E4,5.0E-07/
C  DATA LE,X(1),XM,DELM,R/8.43E-1,3.465E-1,4.965E-1,0.635E-1,
C  #2.04E-1/

DATA LE,X(1),XM,DELM,R/12.645E-1,5.1975E-1,7.4475E-1,0.9525E-1,
#3.048E-1/

```



```

WRITE(*,*)'SELECT THE INPUT PARAMETERS(VELOCITY AND TENSION) UNIT
#SYSTEM.'

WRITE(*,*)'IF VELOCITY IS IN ft./min. AND TENSION IN lb./in. THEN
#TYPE 1, ELSE TYPE 2 FOR VELOCITY IN m/sec. AND TENSION IN N/m.'
READ(*,*)ISYSTEM

C*****
C                               INPUT PARAMETERS
C*****

C  WHETHER SLIP FLOW OR NOT
WRITE(*,*)'FOR NO SLIP CONDITION INPUT 0 OR ELSE INPUT 6.35E-8'
READ(*,*)LAM

C  VELOCITY OF THE FOIL

IF(ISYSTEM .EQ. 1)THEN

WRITE(*,*)'INPUT THE VELOCITY OF THE FOIL/WEB IN ft./min.'
WRITE(*,*)'VELOCITY, V IS CONVERTED TO m./sec. IN THE MODEL'
READ(*,*)V_IN
WRITE(*,*)'INPUT ROLLER SURFACE VELOCITY IN ft./min.'
READ(*,*)VR_IN
V=(V_IN/196.8504)
VR=(VR_IN/196.8504)

C  FOIL TENSION

WRITE(*,*)'INPUT THE FOIL TENSION IN lb./in.'
WRITE(*,*)'TENSION,T IS CONVERTED TO N./m. IN THE MODEL'
READ(*,*)T_IN
T=(T_IN*175.3164556)

ELSEIF(ISYSTEM .EQ. 2)THEN

C  VELOCITY OF THE FOIL

WRITE(*,*)'INPUT THE VELOCITY OF THE FOIL IN m./sec.'
READ(*,*)V_IN
WRITE(*,*)'INPUT THE ROLLER SURFACE VELOCITY IN m./sec.'
READ(*,*)VR_IN
V=V_IN
VR=VR_IN

C  FOIL TENSION

WRITE(*,*)'INPUT THE FOIL TENSION IN N/m.'
READ(*,*)T_IN
T=T_IN
ENDIF

C  TYPE OF WEB/FOIL i.e. NONPOROUS OR POROUS

```

```
WRITE(*,*)'GIVE THE PERMEABILITY FOR THE WEB, 0 FOR NONPOROUS'
WRITE(*,*)'SOME SUGGESTED VALUES ARE: 0.3E-5, 0.52E-5'
READ(*,*)AK
```

C FOIL MASS

```
WRITE(*,*)'INPUT THE FOIL MASS IN Kg./m^2'
WRITE(*,*)'SOME SUGGESTED VALUES ARE: 0.0207,0.0543,0.0695,0.0922'
READ(*,*)M
```

```
ITERP=1
```

C THE ENTIRE DOMAIN ALONG THE ROLLER IS DIVIDED INTO 123 NODES.
 $DELX=(XM-X(1))/(124)$

C "ITERM" IS THE TOTAL NUMBER OF ITERATION TO REACH STEADY STATE.

```
ITERM=INT((XM-X(1))/((V+VR)*DELT))+5000
WRITE(*,*)'ITERM=', ITERM
```

C THE SOLUTION IS PRINTED AFTER EVERY "DELPR" ITERATION.

```
DELPR=((ITERM-5000)/10)
WRITE(*,*)'DELPR=', DELPR
```

C OPENING AN OUTPUT FILE FOR PRINTING THE RESULTS.

```
WRITE(*,*)'GIVE NAME FOR OUTPUT FILE(NOT MORE THAN 15 CHARACTERS)'
READ(*,11)FLNAME
```

```
11 FORMAT(A15)
OPEN(9,FILE=FLNAME)
```

```
Q=(XM-X(1))/DELX
NN=INT(Q)
N=NN+1
WRITE(*,*)'TOTAL NUMBER OF GRID POINTS=',N
```

C CALCULATING THE HEAD PROFILE.

```
DO 2 I=1,N
2 DEL(I)=DELM-R+DSQRT(R**2-(X(1)+(I-1)*DELX-0.5*LE)**2)
```

```
C*****
C INITIALIZING THE VALUES FOR FOIL DISPLACEMENT AND THE PRESSURE
C ALONG THE ROLLER
C*****
```

```
HO=.643*R*(6.*MU*(V+VR)/T)**(2./3.)
WRITE(*,*)'HO= ',HO
PO=PA+T/R
THETA=0.
DO 10 I=1,5
YO=DELM+HO-(R+HO)*(1.-DCOS(THETA))
```

```

XO=.5*LE-(R+HO)*(DSIN(THETA))
10 THETA=DATAN(YO/XO)
AX=X(1)*YO/XO
WRITE(9,*)'XO=',XO,',YO=',YO

DO 20 I=1,N
IF((X(1)+(I-1)*DELX) .GT. XO) GO TO 15
Y(I,2)=(X(1)+(I-1)*DELX)*YO/XO-AX
Y(I,1)=Y(I,2)
II=N-I+1
Y(II,2)=Y(I,2)
Y(II,1)=Y(I,2)
DEL(I)=DEL(I)-AX
P(I)=PA
H(I,2)=Y(I,2)-DEL(I)
H(I,1)=H(I,2)

DEL(II)=DEL(II)-AX
P(II)=PA
H(II,2)=H(I,2)
H(II,1)=H(II,2)
20 CONTINUE

15 II=N-I+1
DO 30 I=1,II
DEL(I)=DEL(I)-AX
Y(I,2)=DEL(I)+HO
Y(I,1)=Y(I,2)
P(I)=PO
H(I,2)=HO
H(I,1)=HO
30 CONTINUE
WRITE(9,*)

```

```

C*****
C SOLVING THE TRANSIENT REYNOLDS EQUATION FOR NEW PRESSURE PROFILE
C*****

```

```

WRITE(*,*)T
C CORRECTING WEB TENSION CONSIDERING THE MASS OF THE WEB

```

```
T=T-M*(V**2)
```

```
WRITE(*,*)T
```

```

WRITE(9,*)T=',',T_IN
WRITE(9,*)V=',',V_IN
WRITE(9,*)VR=',',VR_IN
WRITE(9,*)R=',',R
WRITE(9,*)MASS M=',',M
WRITE(9,*)LAM=',',LAM
WRITE(9,*)AK=',',AK

```

```

N1=N-1
N2=N-2

```

101 ITER=ITER+1

DO 40 I=1,N2
J=I+1

B(I)=(-6.*(V+VR)*MU*H(J,2)/(2.*DELX))-((H(J,2)**3)*P(J)/DELX**2)+
#(H(J,2)**3)*(P(J+1)-P(J-1))/(4.*DELX**2)+3.*(H(J,2)**2)*P(J)
#*(H(J+1,2)-H(J-1,2))/(4.*DELX**2)-6.*LAM*PA*H(J,2)**2/DELX**2+
#6.*LAM*PA*H(J,2)*(H(J+1,2)-H(J-1,2))/(2.*DELX**2)

D(I)=12.*MU*(2*H(J,2)-H(J,1))/DELT+2.*(H(J,2)**3)*P(J)/(DELX**2)
#+12.*LAM*PA*(H(J,2)**2)/(DELX**2)+3.*MU*(V+VR)*(H(J+1,2)-H(J-1,2))
#/DELX+(12*MU*AK*(P(J)-PA))

A(I)=(6.*(V+VR)*MU*H(J,2)/(2.*DELX))-((H(J,2)**3)*P(J)/DELX**2)-
#(H(J,2)**3)*(P(J+1)-P(J-1))/(4.*DELX**2)-3.*(H(J,2)**2)*P(J)
#*(H(J+1,2)-H(J-1,2))/(4.*DELX**2)-6.*LAM*PA*(H(J,2)**2)/DELX**2-
#6.*LAM*PA*H(J,2)*(H(J+1,2)-H(J-1,2))/(2.*DELX**2)

C(I)=12.*MU*H(J,2)*P(J)/DELT

40 CONTINUE

B(1)=0.0
A(N2)=0.0
C(1)=C(1)-
#((-6.*(V+VR)*MU*H(2,2)/(2.*DELX))-((H(2,2)**3)*P(2)/DELX**2)+
#(H(2,2)**3)*(P(3)-P(1))/(4.*DELX**2)+3.*(H(2,2)**2)*P(2)
#*(H(3,2)-H(1,2))/(4.*DELX**2)-6.*LAM*PA*H(2,2)**2/DELX**2+
#6.*LAM*PA*H(2,2)*(H(3,2)-H(1,2))/(2.*DELX**2))*PA

C(N2)=C(N2)-
#((6.*(V+VR)*MU*H(N1,2)/(2.*DELX))-((H(N1,2)**3)*P(N1)/DELX**2)-
#(H(N1,2)**3)*(P(N)-P(N2))/(4.*DELX**2)-3.*(H(N1,2)**2)*P(N1)
#*(H(N,2)-H(N2,2))/(4.*DELX**2)-6.*LAM*PA*(H(N1,2)**2)/DELX**2-
#6.*LAM*PA*H(N1,2)*(H(N,2)-H(N2,2))/(2.*DELX**2))*PA

C UPPER TRIANGULARIZATION

DO 49 I=2,N2
RR=B(I)/D(I-1)
D(I)=D(I)-RR*A(I-1)
49 C(I)=C(I)-RR*C(I-1)

C BACK SUBSTITUTION

C(N2)=C(N2)/D(N2)
DO 59 I=2,N2
J=N2-I+1
59 C(J)=(C(J)-A(J)*C(J+1))/D(J)

DO 69 I=1,N2
J=I+1
P(J)=C(I)

```
PR(J)=P(J)-PA
69 CONTINUE
```

```
PR(1)=P(1)-PA
PR(N)=P(N)-PA
```

```
C*****
C SOLVING THE FOIL EQUATION USING THE UPDATED VALUES FOR PRESSURE
C TO OBTAIN NEW VALUES FOR FOIL DISPLACEMENT AND AIR FILM GAP.
C*****
```

```
DO 79 I=1,N2
J=I+1
BB(I)=-M*V/(2.*DELX*DELT)+M*(V**2)/(DELX**2)-T/(DELX**2)

DD(I)=M/(DELT**2)-(2.*M*(V**2))/(DELX**2)+(2.*T/(DELX**2))

AA(I)=M*V/(2.*DELX*DELT)+M*(V**2)/(DELX**2)-T/(DELX**2)

CC(I)=(P(J)-PA)+(2.*M/DELT**2)*Y(J,2)-(M/DELT**2)*Y(J,1)+
#(M*V/(2*DELX*DELT))*Y(J+1,1)-(M*V/(2.*DELX*DELT))*Y(J-1,1)
```

```
79 CONTINUE
```

```
BB(1)=0.0
AA(N2)=0.0
CC(1)=CC(1)-(-M*V/(2.*DELX*DELT)+M*(V**2)/(DELX**2)-T/DELX**2)*
#(Y(1,1))
CC(N2)=CC(N2)-(M*V/(2.*DELX*DELT)+(M*V**2/DELX**2)-T/DELX**2)*
#(Y(N,1))
```

```
C UPPER TRIANGULARIZATION
```

```
DO 89 I=2,N2
RRR=BB(I)/DD(I-1)
DD(I)=DD(I)-RRR*AA(I-1)
89 CC(I)=CC(I)-RRR*CC(I-1)
```

```
C BACK SUBSTITUTION
```

```
CC(N2)=CC(N2)/DD(N2)
DO 99 I=2,N2
J=N2-I+1
99 CC(J)=(CC(J)-AA(J)*CC(J+1))/DD(J)
```

```
DO 109 I=1,N2
J=I+1
Y(J,3)=CC(I)
H(J,3)=Y(J,3)-DEL(J)
109 CONTINUE
```

```
Y(1,3)=Y(1,1)
Y(N,3)=Y(N,1)
H(1,3)=H(1,1)
H(N,3)=H(N,1)
```

```

C*****
C PRINTING THE SOLUTION i.e. THE AIR FILM THICKNESS AND THE
C PRESSURE PROFILE ALONG THE ROLLER.
C*****

      IF (ITER .GE. ITERP)THEN
      WRITE(9,*)
      WRITE(9,*)'ITER=',ITER
      WRITE(9,*)'AIR FILM GAP, H IS IN m. AND PRESSURE, PR IS IN Pa'
      WRITE(9,*)'VALUES IN PARENS ARE TIME IN msec.(ms.)'

C OUTPUT AIR FILM GAP, H IS IN m. AND PRESSURE, PR IS IN Pa.
      WRITE(9,*)
      WRITE(9,299)ITER*5.E-4,ITER*5.E-4
299 FORMAT(23X,'H(',F5.2,'ms.),'15X,'PR(',F5.2,'ms.)')
      DO 300 I=1,N
300 WRITE(9,*) I, ' ',H(I,3), ' ',PR(I)
      ITERP=ITERP+DELPR
      ENDIF

C*****
      DO 210 I=1,N
      Y(I,1)=Y(I,2)
      H(I,1)=H(I,2)

      Y(I,2)=Y(I,3)
      H(I,2)=H(I,3)

210 CONTINUE

C*****

      IF(ITER .LE. ITERM) THEN
      GO TO 101
      ENDIF
      STOP
      END

C*****
C MECHANICAL AND AEROSPACE ENGINEERING, OSU.
C*****

```

VITA 7

Satyanarayan Kothari

Candidate for the Degree of

Master of Science

Thesis: COMPUTATIONS OF AIR FILMS BETWEEN MOVING WEBS
AND SUPPORT ROLLERS

Major Field: Mechanical Engineering

Biographical:

Personal Data: Born in Raipur, India, On June 16, 1970, the son of Sunderdas Kothari and Shanta Kothari.

Education: Graduated from Holy Cross Higher Secondary School, Raipur, India, in May 1989; received Bachelor of Engineering degree in Mechanical Engineering from Visvesvarayya Regional College of Engineering, Nagpur University, Nagpur, India in July 1993. Completed the requirements for the Master of Science degree in Mechanical Engineering at Oklahoma State University in May, 1996.

Experience: Research Assistant, Department of Mechanical and Aerospace Engineering, Oklahoma State University, Nov. 1994, to May 1996.
Teaching Assistant, Department of Mechanical and Aerospace Engineering, Oklahoma State University, Aug. 1995, to Dec. 1995.
Project Engineer, Ravindra Engineering Pvt. Ltd., Bombay, India, July 1993, to June 1994.

Professional Membership: American Society of Mechanical Engineers and American Society of Heating, Refrigerating and Air-Conditioning Engineers.